DEVELOPING INSTRUMENTATION FOR MULTI-PARAMETRIC INVESTIGATION OF MECHANISMS OF MECHANOSENSITIVITY IN ION CHANNELS

by

Kalpesh V. Upadhye

Bachelor of Technology, Indian Institute of Technology, Mumbai, India, 2002

Submitted to the Graduate Faculty of

Swanson School of Engineering in partial fulfillment

of the requirements for the degree of

Doctor of Philosophy

University of Pittsburgh

2010

UNIVERSITY OF PITTSBURGH

SWANSON SCHOOL OF ENGINEERING

This thesis was presented

by

Kalpesh V. Upadhye

It was defended on

December 18, 2009

and approved by

Sanjeev G. Shroff, Professor, Department of Bioengineering

Tracy X. Cui, Assistant Professor, Department of Bioengineering

Guogyang Li, Assistant Professor, Department of Electrical Engineering

Ratnesh Lal, Professor, Department of Biological Sciences, University of Chicago

Dissertation Director: Lance A. Davidson, Assistant Professor, Department of Bioengineering

DEVELOPING INSTRUMENTATION FOR MULTI-PARAMETRIC INVESTIGATION OF MECHANISMS OF MECHANOSENSITIVITY IN ION CHANNELS

Kalpesh V. Upadhye, PhD

University of Pittsburgh, 2010

Mechanosensitive (MS) channels are implicated in pathologies of the renal and pulmonary systems. Abnormal activity in MS channel reduces cell viability causing a variety of pathologies. MS channels are also responsible for sensation of pain and hearing. Despite the vital importance of MS channels, very little is known about the gating mechanisms of these channels. Attempts to study the mechanisms are severely limited by the lack of suitable instrumentation. A better understanding of the structure-function interaction of MS channels is necessary to find pharmacological leads for the pathologies. Activation data based on indirect activation of MS channels using hypo- or hyper-osmotic solutions or viscous drag is confounded by factors like membrane stretch and cytoskeletal stress. Traditional patch clamp does not allow direct access to the cell by other probes. While a planar patch clamp chip may allow for such access, most of the existing planar patch clamp chips are focused on high throughput screening for pharmaceutical targets and have designs that limit multi-parametric studies.

We present here instrumentation that combines atomic force microscopy with cellular electrophysiology based on planar patch clamp approach. The instrumentation allows multi-parametric studies on single cells and provides unique insights into mechanisms of activation of not just MS channels, but ion channels in general by combining cellular electrophysiology,

optical microscopy and atomic force microscopy. Using HaCaT cells as our model system we have obtained functional maps of distribution MS channels across cell surface. The maps reveal that the distribution of MS channels on HaCaT cells is highly non-uniform and that the channels are present in small clusters instead of dispersed as single entities. Our results using direct mechanical stimulation of single cells reveal that threshold stress level is required in order to activate MS channels and that the stress has a limited spatial range. Investigation of kinetics of the electrical response to direct mechanical stimulation reveals that the MS channels respond to the mechanical signal after a small time lag, which we attribute to the conformational changes necessary while the channel is being gated.

We hope that the insights gained from studying the mechanosensitive channels of HaCaT cells will also advance the understanding of MS channels in general. Apart from opening new avenues in MS channel research, the instrumentation can also be useful in studying the dynamics and gating of ligand gated channels by appropriately tagging the AFM cantilever. With further improvements in the speed of AFM imaging, it will also be possible to observe the gating of channels in real time at molecular scale by imaging the channel on the cell while the channel is being gated.

TABLE OF CONTENTS

LIST OF TABLES

LIST OF FIGURES

PREFACE

"Knowledge is in the end based on acknowledgement." – Ludwig Wittgenstein.

This work represents four years of work that could not have been finished without the constant and unwavering support from the Department of Bioengineering at the University of Pittsburgh.

With profound gratitude, I would like to thank my adviser Dr. Lance A. Davidson for keeping me motivated and guiding me through the last two years, and Professors Harvey S. Borovetz and Sanjeev G. Shroff for making sure that I keep receiving the funds for my research and stipend. I would also like to thank Lynette K. Spataro and Joan L. Williamson for taking care of my administrative as well as financial matters in very friendly and professional manner.

I would like to thank Dr. Hai Lin who accepted me as a graduate student in his lab and advised me for the first three years of my stay with the Department of Bioengineering. This work is based on his ideas and would not have taken shape without his initial inputs. He obtained the seed funds for this project from NIH (R21-EB004474) and the University of Pittsburgh (CRDF and Start-up funds).

I would like to thank all the remaining members of my thesis committee: Dr. Ratneshwar Lal, Dr. Xinyan (Tracy) Cui and Dr. Guangyong Li for their feedback and advice that was crucial to finishing this project in its entirety.

I would like to thank all the professors from the Department of Bioengineering that I have had the pleasure to interact on a personal level, most notably Dr. Partha Roy, Dr. John Patzer, and Dr. Sanford Leuba for enriching discussions and advice about my career plans and future prospects.

I could not have started the project without the help and advice from Dr. Sandy Hu, Mike McDonald, Andy Holmes and Mark Rubin who trained me to use various fabrication and characterization facilities on campus.

The support that Joseph Candiello, my lab-mate, has given for the last five years and especially the last two years has been invaluable. Without his presence and advice, I would never have learned the AFM, nor would have been able to finish this work. The endless discussions ranging from science to sport made life in the lab a pleasure despite the hardships. He not only taught me the ways of Pittsburgh, but also converted me into a devout Steelers fan – something I will definitely cherish all my life.

I would like to thank my friend Stefan Safta, who has been like a brother, for sharing the pleasures and agonies through these years and of course all my friends in Pittsburgh, most notably (and in no particular order) Sangita Suresh, Sagar Joshi, David Montag, Abhishek

Agarwal, Sandeep Urankar, Andrew Feola, Maria Jaramillo, Richard Miller, Matt McHugh, Eli Wasserman, Ian Bellayr, Wesley Sivak, Ishi Ghosh, Morgan Austin, members of the Roy and Shroff labs, the members of Silk Screen film festival, and many others who made Pittsburgh a home away from home. Special thanks to my cousin, Sameer Dhamangaonkar, who has kept me on the edge by constantly sending me intellectually stimulating articles to read.

A special note of thanks to the Singh family: Dr. Mandal Singh, Dr. Madhu Singh and Roopa Singh, and the Murthy family: Dr. Vamadeva Murthy and Mrs. Jayasheela Murthy for giving me a place in their hearts and making me feel a part of their family.

I would not have had the technical wherewithal to design, perform and finish my experiments without the extraordinary educational grounding that I received from the Indian Institute of Technology, Bombay, India.

I wish to dedicate this thesis to my family: Dad, Vinayak Upadhye (Baba) and Mom, Vrushali Upadhye (Aai) for making me who I am and giving me the physical, emotional and spiritual strength to keep striving for excellence in face of hardships. The ever so pragmatic and positive attitude towards life that my father taught me together with the sensitivity infused by my mother have made it possible for me to endure through this arduous endeavor thousands of miles away from home and come out successful.

Finally, the love of my life, Mangala, I thank you for supporting me through, hopefully, the most difficult period of my life.

1.0 INTRODUCTION

Techniques traditionally used to study ion channels involve cellular electrophysiology, molecular biology and pharmacology. One approach commonly used to study mechanosensitive (MS) channels is to use solutions of differing osmolarity combined with intracellular calcium sensitive fluorescent dyes that are activated by calcium entering the cells through the MS channels. Another approach is controlling patch pressures in a micropipette based patch-clamp setting; however, data from controlled negative pressures applied to the patch electrodes is complicated by pipette induced hypo/hyper mechanosensitivity (Hamill and McBride 1997). Despite significant advances in techniques to study mechanosensitive channels, instrumentation that would enable observation of mechanosensitivity under direct mechanical stimuli like membrane deformation and stress has not yet been developed.

In this research, we present instrumentation that will allow multi-parametric investigation of MS channels. We combine cellular electrophysiology, atomic force microscopy and optical microscopy to enable observation of electrical responses of cells under direct mechanical stimuli. We designed and fabricated a silicon dioxide based planar patch clamp chip and microfluidics to integrate atomic force microscope (AFM) to directly stimulate cells mechanically while simultaneously performing whole-cell recordings of ionic current from the cells. We have chosen TRPV4 channels as our model for mechanosensitivity because of the ubiquity of TRPV4

channels in various organs in humans. HaCaT keratinocytes, because of the predominant presence of TRPV4 channels, are our choice of cells.

TRPV4 has been observed to be sensitive to cell volume changes (Nilius, Prenen et al. 2001), changes in viscous load (Andrade, Fernandes et al. 2005) and shear stress (Taniguchi, Tsuruoka et al. 2007) without displaying stretch sensitivity. Other studies suggest that TRPV4 is not directly MS but instead is coupled to one or more MS enzymes, most notably phospholipase A_2 (PLA_2) (Watanabe, Vriens et al. 2003). Evidence suggests that, irrespective of the actual mechanism, the local membrane properties play an important role in activation of MS channels; either through directly influencing the channel upon stretching by exerting tensional forces directly on the channel molecule (Ingber 2006), or through inducing conformational changes because of local modification of lipids surrounding the channel. We hope that our findings will lead to a better understanding of the role of lipid bilayer in activation of MS channels in general and TRPV4 channels in particular.

The research was divided into three aims:

Aim 1: Design and fabricate a planar patch clamp chip. Fertig et al (Fertig, Blick et al. 2002) made a major advance by fabricating a planar chip to work as a micropipette in patch clamp experiments making patch clamp more amenable to integration with other techniques requiring access to the cell. We improve the design of the planar patch clamp chip to make it more versatile and compatible with other powerful techniques such as fluorescence microscopy and scanning probe microscopy.

Aim 2: Integrate the planar patch clamp chip and the related fluidics assembly with an atomic force microscope and an optical microscope in order to simultaneously image and/or stimulate a single cell using an atomic force microscope (AFM) while recording from it in whole-cell patch clamp mode. Integrating patch clamp and atomic force microscopy techniques enables us to apply direct mechanical stimuli to cells while recording whole-cell current.

Aim 3: Investigate the effect of local bilayer curvature on activation of TRPV4 channel. We use direct mechanical stimuli using an atomic force microscope (AFM) cantilever to introduce changes in lipid bilayer curvature in HaCaT cells expressing TRPV4 channels while recording from the cells. The apparatus allows us to investigate the current response under various voltage and bilayer curvature conditions.

By combining AFM and fluorescence imaging with electrophysiology, our instrumentation allows us to expose cells to more complex and locally focused stimuli that so far have been incompatible with whole cell patch clamp techniques. The instrumentation gives us (and the scientific community) the capability to perform unique experiments on mechanisms and dynamics of ion channels in general and MS channels in particular.

1.1 THESIS OUTLINE

In chapter 2 we review a brief background on the current understanding of mechanosensitive (MS) channels as well as the current state-of-the-art in planar patch clamp chips. We also briefly review atomic force microscopy and its versatility in investigating various

biological phenomena. We outline how integrating planar patch clamp and AFM would benefit ion channel research in general and MS channel research in particular.

In chapter 3 we detail the design and fabrication of a silicon/silicon dioxide based planar patch clamp chip as well as the microfluidics necessary to enable its integration with an atomic force microscope. The design constraints are based on the available instrumentation which includes the AFM, the inverted reflecting optical microscope and a patch clamp amplifier. The final instrumentation is capable of simultaneous optical/fluorescence imaging while applying direct mechanical stimulus using an AFM cantilever to a whole-cell voltage clamped live cell.

Chapter 4 describes the results of characterization of the planar patch clamp chip and some proof-of-concept experiments to show that the chip and microfluidics is on par with other planar patch clamp techniques. We show the tests for giga-ohm seals, capability intra- and extra-cellular solution exchange as well as compatibility with optical microscopy techniques.

In chapter 5, we describe our experiments for investigating mechanisms of mechanosensitivity of MS channels in HaCaT cells by using the AFM cantilever to “poke” the cells at different depths, with varying force at a variety of rates while the cell is voltage-clamped at different voltages. This truly illustrates the power and versatility of the instrumentation in performing multi-parametric investigations on live cells in order to study a wide variety of ion channels including specifically MS channels.

Chapter 6 summarizes the project and discusses the implications of the results as well as the future of this technology and potential new avenues in which this instrumentation can be used.

2.0 RESEARCH BACKGROUND

In this chapter we provide a brief overview of the patch clamp technique after summarizing the current understanding of mechanosensitive (MS) channels and the techniques used to study them while introducing the need for a newer paradigm in patch clamp experiments – the planar patch clamp. This is followed by a review of the current state-of-the-art in planar patch clamp chips. We also briefly review atomic force microscopy and its versatility in investigating various biological phenomena. We conclude the chapter by outlining how integrating planar patch clamp and AFM would benefit ion channel research in general and MS channel research in particular.

2.1 ION CHANNELS

All living cells have a plasma membrane that separates their interior compartments and the internal organelles from the surrounding environment. The membrane consists of a lipid bilayer that prevents the passage of ions and macromolecules across the cell boundaries. Specialized proteins in the cell membrane, such as ion-channels and other transporters, mediate the transport of ions and small molecules including sugars and amino acids, in and out of the cell. A number of different ion channels are present on the cell membrane, including passive pores, as well as voltage sensitive, ligand-gated, and mechano-sensitive gating proteins (Hille

2001). Ion channels help maintain the crucial ionic balance inside the cell and they mediate communication and the electrical signaling in cells/tissues including heart, nervous system, and other organs via ionic currents conducted through various ion-channels. Ion channels have also been important targets for therapeutic intervention for a wide variety of diseases (Cahalan and Chandy 1997). The focus of this study, however, is the mechanosensitive (MS) ion channels.

Mechanosensitive ion channels are the molecular switches, responsible for mechano-electrical transduction in cells. These ion channel proteins are embedded in the cell membrane and respond to various mechanical stimuli to the membrane by selectively conducting ions into or out of the cell, thus, changing the membrane permeability. In 1987 Martinac, et al., discovered the origin of osmoregulation in *E. Coli* (Martinac, Buechner et al. 1987) as pressure-activated ion channels. They concluded that these ion channels (i) are activated by positive or negative pressure, (ii) are also voltage sensitive, (iii) have large conductance and (iv) selective for anions over cations. Sukharev, et al., were the first to identify the molecular origins of fast osmoregulatory responses in bacteria (Sukharev, Martinac et al. 1993) and to functionally reconstitute the solubilized ion channels in liposomes leading them to infer that these channels are gated by tension transduced via the lipid bilayer. They identified two distinct ion channels; one with large conductance activated by higher negative pressures (later named as mechano-sensitive channel of large conductance, MscL) and one with small conductance (later named as mechano-sensitive channel of small conductance, MscS) activated by lower negative pressures which would cause the bilayer to contract. Hamill and McBride used pressure clamp on Oocytes to study the pressure dependence of gating of mechanosensitive ion channels (McBride and Hamill 1992; McBride and Hamill 1993). In a later study (Hamill and McBride 1997) the same

group concluded that the pressure clamp technique may induce excessive membrane stress during or after seal formation leading to an increase or decrease in native mechanosensitivity. Cui, et al., soon after characterized both MscL and MscS in *E.Coli* (Cui, Smith et al. 1995). Later, Kloda and Martinac identified the sequence from bacterial MS channels that is conserved in prokaryotic MS channels (Kloda and Martinac 2001) opening up the whole new field of prokaryotic MS channels.

A putative vertebrate MS channel, later to be named TRPV4, was identified by Liedtke, et al. (Liedtke, Choe et al. 2000). The group found that invertebrate homologue of this channel was necessary for nose touch sensation in *C. elegans* (Liedtke, Tobin et al. 2003). TRPV4, a member of the vanilloid sub-family of the TRP superfamily of proteins, has since then found to be expressed in a wide range of sensory as well as non-sensory cells including inner-ear, skin, trachea, kidney epithelial cells, and so on. Mice lacking TRPV4 show abnormal osmotic regulation (Liedtke and Friedman 2003). TRPV4 is also an interesting system to study because the channel can be activated by a variety of mechanisms, from chemical to physical stimuli. TRPV4 channels have been observed to sense changes in mucosal viscosity (Andrade, Fernandes et al. 2005), pressure (Suzuki, Mizuno et al. 2003; Tabuchi, Suzuki et al. 2005), fluid shear (Jia, Wang et al. 2004; Reiter, Kraft et al. 2006; Hartmannsgruber, Heyken et al. 2007; Taniguchi, Tsuruoka et al. 2007; Wu, Gao et al. 2007), osmolarity (Alessandri-Haber, Yeh et al. 2003; Alessandri-Haber, Joseph et al. 2005; Mangos, Liu et al. 2007), cell volume (Nilius, Prenen et al. 2001; Becker, Blase et al. 2005), temperature (Guler, Lee et al. 2002; Watanabe, Vriens et al. 2002; Chung, Lee et al. 2003) and chemicals like phorbol esters (Watanabe, Davis et al. 2002) and anandamide (Watanabe, Vriens et al. 2003). Recent evidence suggests that TRPV4 channel

has a role to play in processes as diverse as regulation of unloading-induced bone loss (Mizoguchi, Mizuno et al. 2008) and visceral hyperaglesia (Sipe, Brierley et al. 2008).

2.1.1 Prokaryotic MS Channels

Despite the ubiquity and vital importance of MS channels, very little is known about the mechanisms of modulation of these channels. Evidence suggests that there might be multiple mechanisms involved in this process. Local membrane properties play an important role in activating bacterial MS channels, which are the most extensively studied MS channels so far. In case of bacterial MS channels (MscL and MscS), the constitution of the bilayer membrane affects the curvature of the membrane, thereby determining the conformation of these channels (Perozo, Kloda et al. 2002).

Prokaryotic MS channels (MscL and MscS) have been extensively studied. It is generally thought that MS channels gate in response to difference in pressure across the membrane that causes distortion of the bilayer. Blount et al (Blount, Sukharev et al. 1996) and others (Okada, Moe et al. 2002; Sukharev 2002) have shown that MscL and MscS are both active even after reconstitution in planar lipid bilayers indicating that both these channels respond directly to membrane stress and do not need redundant auxiliary proteins for gating. MscS is activated at relatively low tensions of about 5.5 dyne/cm with a conductance of about 1 nS (Sukharev 2002) whereas, MscL is activated at considerably higher tensions (about 10 dyne/cm) with typical conductance values around 3.5 nS (Chiang, Anishkin et al. 2004). MscS activation depends on the rate of applied stimulus rather than the actual value of the stimulus as evident from responses

to abrupt pressure changes versus slow pressure changes and inactivation under sustained pressures (Akitake, Anishkin et al. 2005). MscL does not show such inactivation. While MscS has quite a complex structure and mechanism, MscL has a relatively simple gating mechanism. MscL is postulated to have two gates – a transmembrane (TM) gate which acts as the main gate and another cytoplasmic gate composed of five α-helical S1 segments at the N-termini (Sukharev, Betanzos et al. 2001; Sukharev, Durell et al. 2001). According to the model proposed by Betanzos et al (Betanzos, Chiang et al. 2002) the TM gate acts as the pressure sensor. This gate permits initial partial opening of the channel on application of pressure while the cytoplasmic gate allows for full activation of the channel; the applied pressure is transmitted to the S1 segments through the flexible linkers and pulls them apart. Recent molecular dynamics simulations on the MscL-lipid system (Jeon and Voth 2008) underline the importance of hydrophobic forces and asymmetry in the bilayer in its activation process.

2.1.2 Eukaryotic MS Channels

In eukaryotic cells, however, existence of excess membrane and a highly flexible submembranous CSK makes it physically unlikely for the mechanical stresses to be transferred to MS channels through the submembranous CSK or the bilayer membrane (Ingber 1997). All the forces would be dissipated by the submembranous CSK or the bilayer membrane. In contrast, tethering of the channels via integrin or similar molecules might result in local stiffening of the bilayer and submembranous CSK leading to focusing of the stresses sufficient to induce conformational changes in the channel. It is also possible that the linkages between the MS channels and submembranous CSK and/or extracellular matrix elements localize and immobilize

the channels so as to allow transfer of stresses from the bilayer membrane or submembranous CSK to the channel. The tethering might simply be a way to stop the MS channels from drifting in the bilayer membrane with the lipid rafts because of the applied stress. Two models have been suggested for eukaryotic MS channel activation (Hamill 2007):

- *Bilayer model:* This model proposes that changes in the lipid bilayer tension bring about a conformational change in the MS channel resulting in activation of the channel. The evidence for this mechanism is provided by patch clamp experiments performed on liposomes with reconstituted MS channel proteins (Blount, Sukharev et al. 1996; Okada, Moe et al. 2002). Fig. 2.1 (a) shows a cartoon depiction of the bilayer model of MS channel activation.
- *Tether model:* According to this model, mechanical stress is transmitted to the MS channel through the submembranous cytoskeleton (CSK) or components of the extra-cellular matrix to which the MS channels are tethered. Fig. 2.1 (b) shows a cartoon depiction of this mechanism. Although, direct evidence relating to how certain MS channels are activated by molecules in the CSK and/or extracellular matrix is lacking, abolition of the response to mechanical stimuli after treatment with cytochalasin D, which disrupts the connectivity of internal actin CSK without depolymerization of T-actin, in some cells suggests that this may be the mechanism for MS channel activation.

Ankyrin repeats are a conserved feature in MS channels. Ankyrin domains in integrin-linked kinase seem to be important for binding with integrin in focal adhesion. Thus, it may be possible that MS channels are dependent on these adaptor proteins for activation. Evidence from some of the channels, notably TRAP1 (Corey, Garcia-Anoveros et al. 2004) and BK (Tang, Xu et al.

2003) channels, suggests that observed changes in channel gating are likely mediated by adaptor proteins as well as bilayer tension. There is also strong evidence that lot of the same channels also respond to direct membrane when recorded from reconstituted liposomes. This suggests that, in actuality, one of the two or even both mechanisms might be at play in activating MS channels depending on the specific cell and other conditions.

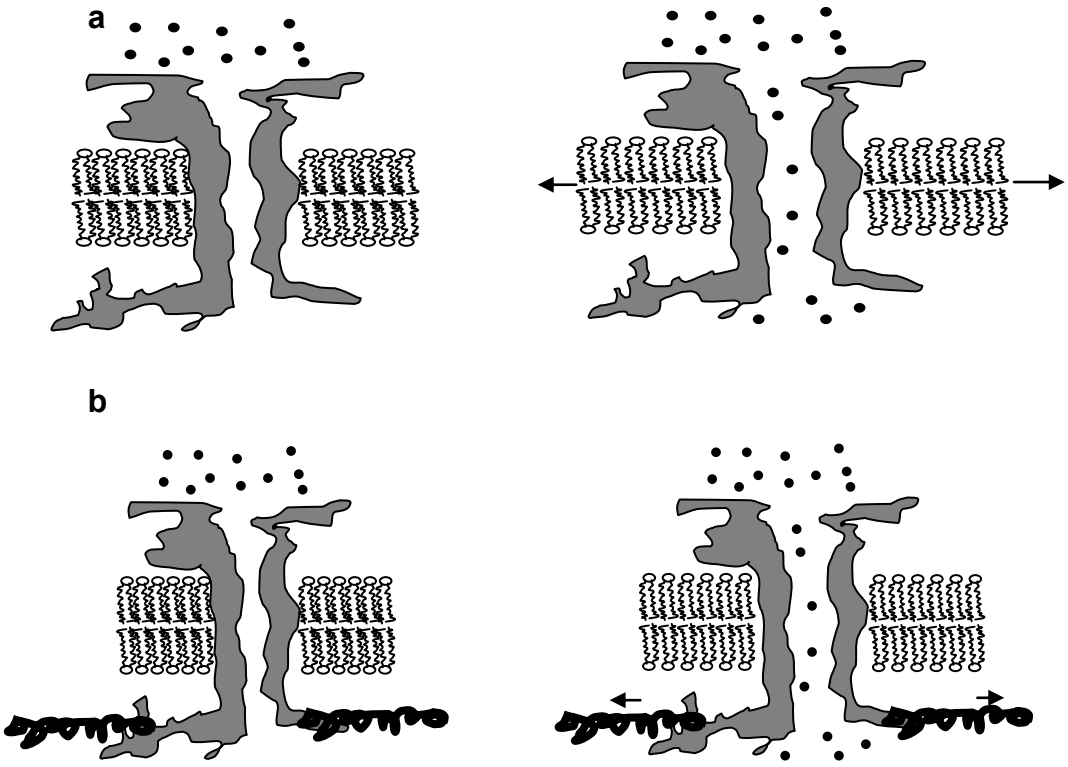

Figure 2.1. Cartoon depiction of models of mechanotransduction. (a) the bilayer model: Distortion in the bilayer membrane induces conformational changes in the channel sufficient to activate the channel. Arrows show the direction of the tensional forces and the left panel shows a closed channel and the right one shows an open channel; (b) and tethered model: The tensional forces are transmitted directly from the submembranous cytoskeleton (CSK) to which the MS channel is tethered. The forces activate the channel by inducing conformational changes by tugging on the cytoplasmic domains of the channel (adapted from (Ingber 2006)).

Activation of TRPV4 channels by physical stimuli, point to TRPV4 being a mechanosensitive channel, but the exact mechanism of activation is still largely unknown. Drawing analogy from the bacterial MS channels, it is thought that TRPV4 channels are activated through conformational changes induced by changes in local curvature of the cell membrane. This hypothesis is also supported by observations that some of the chemical activators of TRPV4 channels are lipids which can easily incorporate in the bilayer membrane, and because of their structure, might induce change in the local curvature of the bilayer.

The availability of suitable tools remains a major hurdle in testing this hypothesis. Some of the techniques used to study and manipulate MS channels include (Hamill 2007):

(i) Electrophysiology and manipulation of MS channels by reconstituting them into planar bilayers or vesicles. This method has been very successful in studying bacterial MS channels but has certain limitations in terms of the amount of lipid that can be used to study and how that affects the channel characteristics;

(ii) Use of cell swelling via exposure to hypoosmotic extra-cellular media (Bourque, Oliet et al. 1994; Schoenmakers, Vaudry et al. 1995; Waniishi, Inoue et al. 1997). The difficulty in this technique is in estimating the effect of change in volume on membrane tension. Other confounding factors like activation of intracellular signaling pathways caused by reduction in ionic strength of cytoplasmic ions and macromolecules that make it difficult to separate the stretch component from these other factors;

(iii) Use of magnetic micro-beads to apply controlled forces to the membrane (Hughes, El Haj et al. 2005; Hughes, McBain et al. 2007). This technique allows studies on the role of mechanical forces in gating of MS channels. Parameters such as area of cell membrane

subjected to the force induced by the bead, cell shape and value of the force applied to the bead need to be estimated when using this technique since one cannot measure these parameters.

(iv) Use of pipettes, styluses or thin carbon fibers to press on the cell (Xian Tao, Dyachenko et al. 2006; Hamill 2007) combined with the use of fluorescent dyes to estimate the ionic currents. Although compression of cell in this manner activates MS currents, one major issue in this technique the estimation of the stress distribution which can be very complicated under compression. Quite like in (iii), quantitative results are difficult to obtain in these studies.

One approach to investigate the mechanism of mechanosensitivity in MS channels would be direct mechanical stimulation in concert with whole-cell patch clamp. Although mechanical stimulation of cells is employed in combination with molecular biology and calcium signaling measurements, electrophysiology remains the best available method capable of single channel and whole-cell current measurements. Despite the well established tools for electrophysiology, the stress states of the membrane before and during attachment to patch-pipettes are ill-understood. Osmotic swelling or other similar perturbations to cell membrane introduce stresses whose distribution is also poorly understood.

2.2 PATCH CLAMP

The most powerful tool for studying ion-channel properties is the “patch-clamp” technique (Neher and Sakmann 1976). In conjunction with molecular biology techniques used to

modify the expression of ion channels in a cell the patch clamp technique has, over the years, been used to glean many insights into the mechanisms underlying ion channel activity. Neher and Sakmann (Neher and Sakmann 1976; Neher and Sakmann 1976) originally developed the patch clamp technique to resolve currents in cell-attached patches of membrane of frog skeletal muscle through single acetylcholine-activated channels. The invention of patch clamp method earned a Nobel Prize (1991) and paved the way for molecular electrophysiology.

Central to the patch clamp technique is a glass micropipette formed by carefully heating and pulling a small glass capillary tube to get the diameter at the tip to about 1-2 μm. This glass micropipette is gently pressed onto the cell membrane and slight suction is applied to form a seal between the membrane and the micropipette tip with seal resistance larger than a giga ohm – the so-called gigaseal. Once the gigaseal is formed, the ion channels in the section of membrane within the opening of the pipette tip provide the electrical connection between electrode buffer from the micropipette and the inner side of the cell. This configuration called the "cell-attached" patch clamp is usually the first step in getting other configurations (Hille 2001).

2.2.1 Patch Clamp Configurations

Patch clamp configurations can be divided into two general categories – the “intact-cell” (cell-attached, whole-cell and perforated patch) configurations and the “excised patch” (inside-out and outside-out) configurations. Since the number of channels under study are on the order of one, the “cell-attached” and both “excised patch” configurations are sometimes referred to as single channel recordings. On the other hand, the “whole-cell” and the “perforated patch”

configurations allow the study of the electrical behavior of the entire cell membrane. The list of various patch clamp techniques is as follows (fig. 2.2):

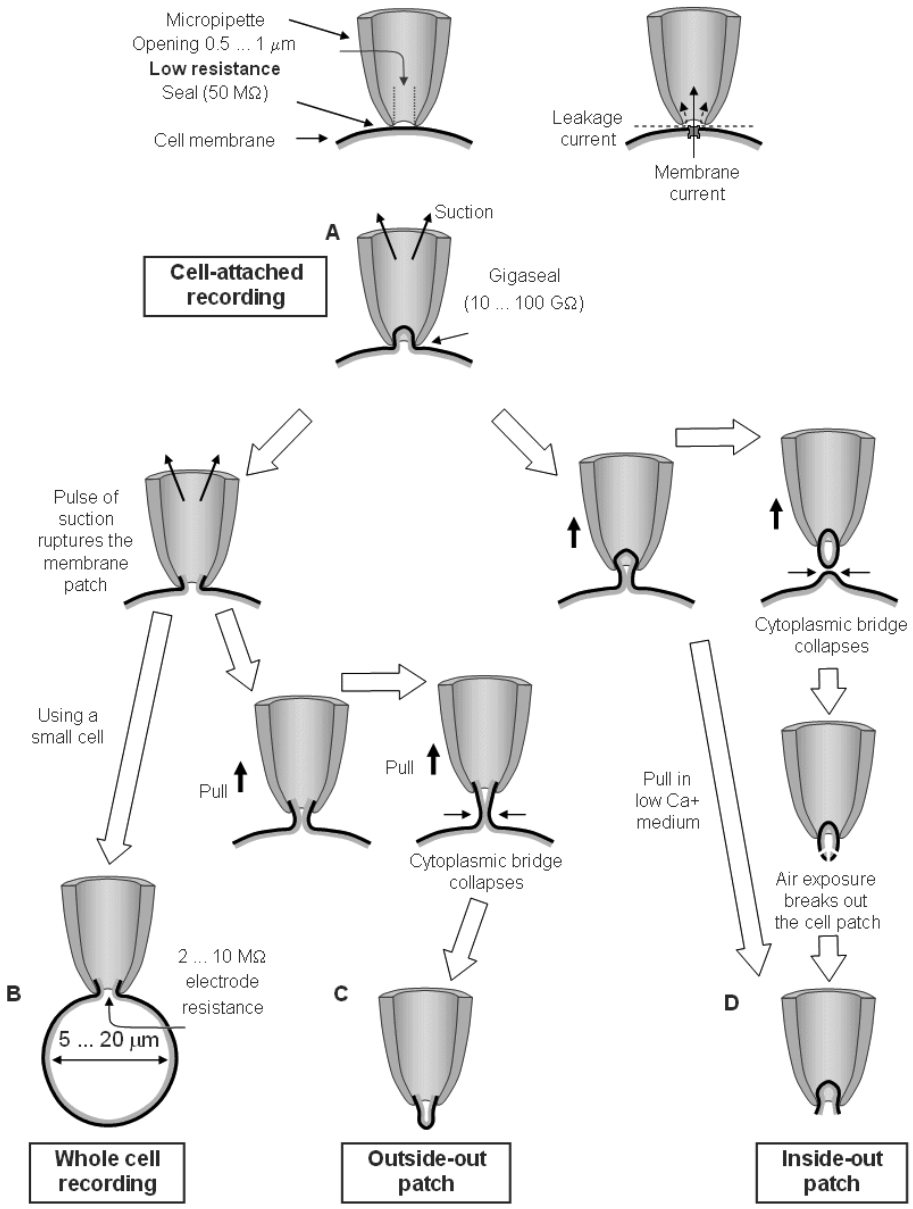

Figure 2.2. Patch clamp configurations. (a) intact-cell configurations include the "cell-attached", the "whole-cell", and the "perforated patch" (b) excised patch configurations include the "inside-out" and the "outside-out" (http://www.bem.fi/book/04/04x/0427x.htm)

- “Cell-attached”: The configuration immediately following the gigaseal is the “cell-attached” configuration. It is essentially the first step in any patch clamp experiments and all other configurations are necessarily derivatives of this configuration. It allows the study of the channels from the small patch of membrane within the micropipette tip.
- "Inside-out" configuration: This configuration is so named because the intracellular surface of the patch membrane is exposed to the external media. The micropipette is quickly withdrawn from the cell to rip the patch of membrane after the gigaseal is obtained to arrive at the inside-out configuration. One uses this configuration when the experiments involve manipulating the environment affecting the intracellular domains of the ion channels.
- “Whole-cell” configuration: This configuration is obtained, after the gigaseal is attained, by applying a sharp suction or voltage pulse to rupture the patch membrane that is inside the pipette opening. This connects the buffer inside the pipette to the intracellular space causing the soluble intracellular contents to slowly diffuse into the buffer of the pipette. Therefore, the pipette buffer properties (pH, molality, ionic concentrations, etc.) must match the properties of cytosolic contents as closely as possible. The whole-cell configuration is used when the experiments involve measuring currents through membrane channels of the whole cell.
- "Outside-out" configuration: To obtain this configuration, after the gigaseal, the pipette is slowly withdrawn from the cell so that the patch is torn off the cell. Then the patch fuses to form a tiny liposome at the end of the pipette, exposing the outside of the membrane to the external buffer. The “outside-out” configuration provides the researcher with opportunities to examine the properties of single ion channels outside of the cellular environment.
- “Perforated patch” configuration: The “perforated patch” configuration is obtained by introducing small amounts of an antibiotic, such as nystatin, or amphotericin B, into the pipette

after the gigaseal is formed. The antibiotic forms non-selective large conductance pores in the membrane, thus, giving electrical access to the inside of the cell. While this configuration has the advantage of keeping the cellular contents intact, it suffers from two key disadvantages: (a) higher access resistance causing a decrease in current resolution and magnification of recording noise, and (b) since the antibiotic reaches the cell only by diffusion through the micropipette, there is a significant time lag between application of the antibiotic and formation of the "perforated patch". This naturally results in reduction in the time available for experiment before the cell dies.

2.3 PLANAR PATCH CLAMP

Most of our knowledge of ion channel proteins is owed to micropipette based patch clamp techniques; however, this method has several limitations:

- Micromanipulation requires considerable skill and is time consuming.
- The system becomes very sensitive to mechanical vibrations.
- Intra-cellular buffers cannot be exchanged to change the conditions in real-time.
- Micropipette creates steric hindrance for approaching the cell by another probe, for instance, of a scanning probe microscope.

Some of these limitations have restricted significant advances in our understanding of MS channels. One of the key limitations in performing single channel recordings on MS channels, especially in live cells, is that even though pressure in the pipette can be controlled precisely, local stresses on the membrane are not known. Since the membrane itself is inhomogeneous in

content and stresses existing in the process of seal formation remain unknown and unaccounted for. The pre-stressed state may lead to wrongly identifying some channels as stretch inactivated channels, since the stress on the membrane might reduce initially if the applied stress is opposite in nature to the already existing pre-stress (Hamill and McBride 1997). Another method used to study MS channels was to use two pipettes – one of which is used for whole-cell recording and the other for stretching the cell. This is a difficult implementation and works only on specific cell types (Davis, Donovitz et al. 1992; Kamkin, Kiseleva et al. 2003; Kamkin, Kiseleva et al. 2003; Kamkin, Kiseleva et al. 2005). Similar methods using glass styluses and thin carbon fibers have also been used to stretch the cells and measure whole-cell currents to study MS channels.

Recently, Fertig, et al (Fertig, Blick et al. 2002) designed and fabricated a glass based chip in an attempt to overcome some of the limitations of patch-clamp technique. The method of fabrication involved the use of high energy gold ions to generate a crystal defect track in quartz resulting in a faster etch rate by hydrofluoric acid along the track (Fertig, Meyer et al. 2001). Since then, the on-chip approach has been attempted by several groups that have developed planar patch clamps in the form of a micron sized aperture in a microfabricated chip, using different materials such as quartz (Fertig, Blick et al. 2002; Fertig, George et al. 2003; Xu, Guia et al. 2003) , silicon (Stett, Bucher et al. 2003; Pantoja, Nagarah et al. 2004) , silicon nitride (Schmidt, Mayer et al. 2000), Teflon (Mayer, Kriebel et al. 2003) and polydimethyl-siloxane (PDMS) (Klemic, Klemic et al. 2002; Ionescu-Zanetti, Shaw et al. 2005). Recently, non-planar forms of multiple patch chips made of PDMS have been developed that allow simultaneous patch recording from multiple cells and fluorescence microscopy imaging (Ionescu-Zanetti, Shaw et al. 2005; Chen and Folch 2006; Lau, Hung et al. 2006). The PDMS-based planar

devices were built using a micromolding process (Klemic, Klemic et al. 2002), whereas quartz, silicon and silicon nitride based planar patch clamps were made using semiconductor fabrication methods. Compared to glass pipettes, planar patch clamps can have significantly better electrical characteristics due to their lower serial resistance and capacitance. Furthermore, fabrication of planar patch clamp chips involves batch processing techniques used in semiconductor industry resulting in highly consistent devices. Sigworth and Klemic (Sigworth and Klemic 2005) provide a good review of the planar patch clamp technologies. Figure 2.3 shows some of the devices reported in the literature.

The planar patch clamp chips fabricated from glass (Fertig, Blick et al. 2002) have so far been the most successful of the designs mentioned above, in terms of electrical recording. Glass has excellent optical properties but the etching method introduces a tapered aperture throughout the depth of glass substrate inducing a significant optical distortion resulting from the interference from varying glass thickness. This leaves the glass based chips at a disadvantage when integrating with optical microscopy techniques. Planar patch clamp chips made of silicon are opaque and hence compatible with only reflected light microscopy techniques and limit access to the cell by another probe like the cantilever of an atomic force microscope. Silicon nitride has excellent optical and dielectric properties however; giga-ohm seals have not been demonstrated in silicon nitride based chips. PDMS based chips have shown some promise, but the designs do not allow for access to the cell.

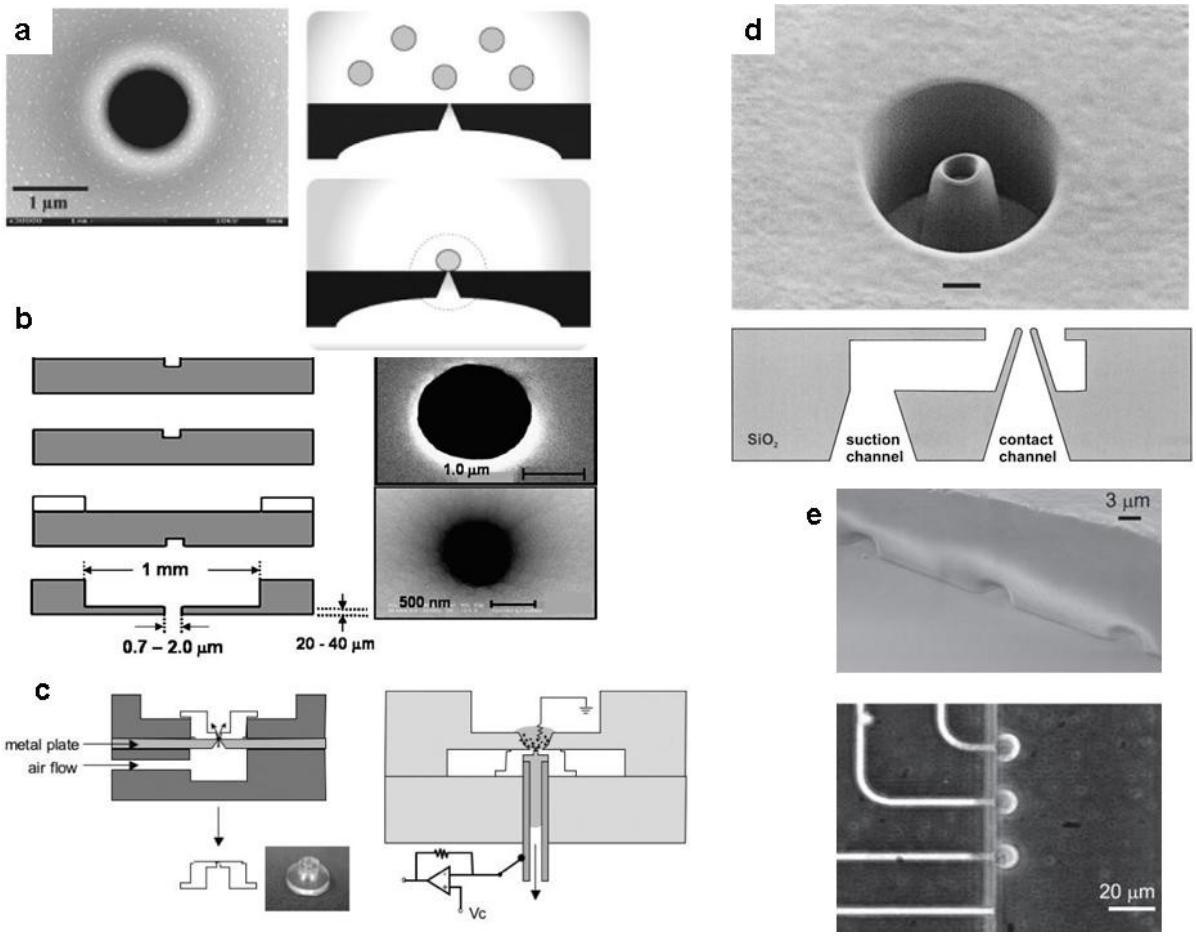

Figure 2.3. Various on-chip patch clamp devices: (a) Scanning electron microscope (SEM) image of the glass chip from the Fertig group (Fertig, Blick et al. 2002) and a schematic of the recording process. (b) Schematic of the fabrication process and SEM images of silicon-based patch-clamp chip by Pantoja et al. (Pantoja, Nagarah et al. 2004). (c) Planar patch clamp device made from polymethyl dioxysilane (PDMS) by Klemic et al. (Klemic, Klemic et al. 2005) using air molding fabrication process; schematic of fabrication process and measurement process. (d) SEM image and cross-section of the CytoPatch^{TM} chip made of quartz by Cytocentrics CCS GmbH (Stett, Burkhardt et al. 2003); the scale bar indicates 1 µm. (e) Schematic and optical microscope images of the multi-cell electrophysiology microfluidic platform fabricated by Ionescu-Zanetti et al in PDMS (Ionescu-Zanetti, Shaw et al. 2005).

2.4 ATOMIC FORCE MICROSCOPY

Some of the issues in estimating stress distribution in force studies of MS channels can be remedied by using an atomically sharp tip like that of an Atomic Force Microscope (AFM).

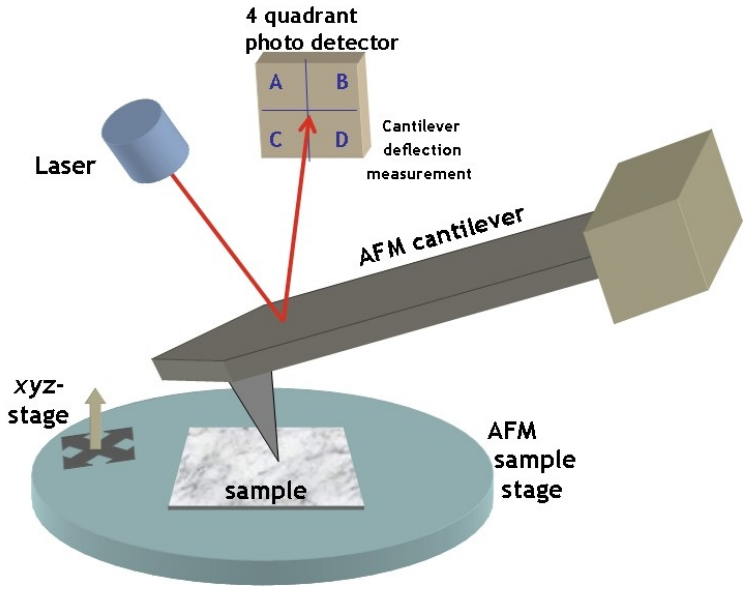

Figure 2.4. Atomic force microscope setup: The deflection of the cantilever is measured by reflecting a laser beam from the top side of the cantilever while it is scanning over the surface of the sample mounted on a piezo-activated XYZ stage. (Source: Opensource Handbook of Nanoscience and Nanotechnology)

The AFM evolved from the scanning tunneling microscope developed by Gerd Binning and Heinrich Rohrer in the 1980's; a development that earned them the Nobel Prize for Physics in 1986. The basic working principle of an AFM is not unlike that of an old fashioned gramophone (or a record player) in that it uses a sharp stylus to measure the indentations on a surface. The difference however is the high level of sophistication and sensitivity of the AFM. Instead of the gramophone pin, the sensing device in an AFM consists of an extremely sharp

micro-cantilever typically fabricated from silicon or silicon nitride. The radius of curvature at the tip of an AFM cantilever is on the order of nanometers. This cantilever tip can be scanned over the sample using piezoelectric actuators with sub-nanometer accuracy. As the tip is brought in proximity of the sample, forces between the tip and the sample cause the cantilever to deflect according to the Hooke's law in the small deflection regime. The nature of the forces between the tip and the sample may vary depending on the sample, the cantilever type and scanning mode, and include van der Waals forces, capillary forces, magnetic forces, chemical bond, and electrostatic forces and so on. The most common method of measuring the deflection of the cantilever involves measuring the deflection of a laser spot reflected from the top surface of the cantilever using an array of photodiodes (Fig. 2.4).

AFM has been used to image and manipulate a variety of surfaces and materials. But, for biological studies, the primary advantage of AFM stems from the sub-nanometer resolution it can provide in physiological conditions (in air or liquid buffers). AFM has been used to image single polymer molecules (DNA, proteins and other macromolecules) (Roiter and Minko 2005) supported lipid bilayer (Larmer, Schneider et al. 1997), study protein interactions and dynamics (Lin, Clegg et al. 1999), and to measure mechanical properties of tissues by indenting the tissue with known forces under physiological conditions (Candiello, Balasubramani et al. 2007; Merryman, Liao et al. 2007). AFM can used to apply forces as small as 1 nN and perform indentations on live cells over nanometer areas on the order of nanometers at rates from 10nm/s to 10μm/s. AFM imaging of the plasma membrane of live cells is reasonably common and has provided useful information about ion channels, cellular processes and dynamics (Lal, Kim et al. 1993; Lal and Lin 2001; Lin, Bhatia et al. 2001; Quist, Chand et al. 2007). AFM images of

excised membrane patches spanning the opening of a glass pipette have been obtained (Horber, Mosbacher et al. 1995; Larmer, Schneider et al. 1997). Movement of the cell membrane in response to voltage stimuli has been shown in pipette based patches (Zhang, Keleshian et al. 2001) as well as in chip-based patches (Pamir, George et al. 2007). But so far, no one has used AFM to provide controlled mechanical stimuli as a compliment for electrophysiology in studying activation dynamics of ion channels in live cells, especially for mechanosensitive ion channels.

Thus far, primary limiting factor preventing the use of AFM in conjunction with patch-clamp on live cells is the limited access to a patched cell. The steric hindrances of the conventional patch clamp apparatus limit physical access to the cell by another probe. We have, therefore, designed a patch clamp chip assembly that will be compatible with AFM by allowing approach access to the cell for the AFM cantilever.

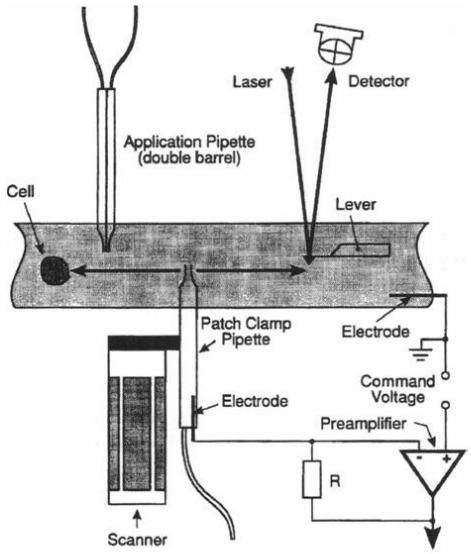

Figure 2.5. Schematic of the apparatus used for obtaining AFM images of excised membrane patches spanning the opening of a glass pipette (Horber, Mosbacher et al. 1995).

3.0 FABRICATION OF PLANAR PATCH CLAMP SYSTEM

In this chapter we detail the design and fabrication of a silicon/silicon dioxide based planar patch clamp chip as well as the microfluidics necessary to enable its integration with an atomic force microscope. The design constraints were based on the equipment available in our lab including the AFM (Asylum Research), the inverted reflecting optical microscope (Olympus) and a patch clamp amplifier (A-M Systems). The final instrumentation is capable of simultaneous optical/fluorescence imaging and application of direct mechanical stimulus using an AFM cantilever to a voltage clamped live cell.

3.1 DESIGN CONSTRAINTS

Planar patch clamp chip based approach to electrophysiology has the potential to take the field of MS channel research to the next level of understanding. Our objective was to design a planar patch clamp chip compatible with high resolution optical and scanning probe microscopy. Our constraints were dictated by the necessity to keep the patching (top) surface transparent and flat. After a careful study of all the previous designs and our needs we decided on a chip design that would have a 1 μm diameter pore in a transparent membrane on top of a substrate and

accessible from the bottom side of the substrate (for cross section, see Figure 3.1). This would in essence act like an inverted micropipette with a 1 µm opening.

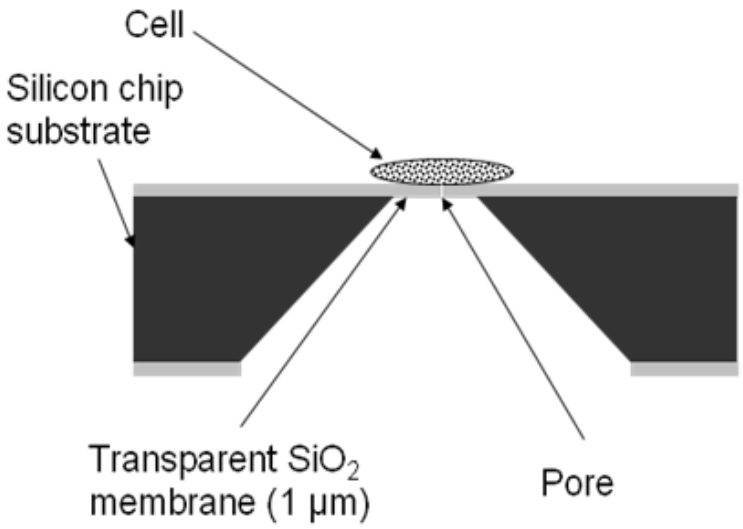

Figure 3.1. Cross-section of the planar patch clamp chip design

The MEMS fabrication facilities including electron beam lithography and reactive ion etching at the Petersen Institute of Nanoscience and Engineering, University of Pittsburgh give us access to the "silicon fabrication toolbox". Since, glass or quartz pipettes form excellent gigaseals with cell membranes (Opsahl and Webb 1994; Suchyna, Markin et al. 2009), we chose silicon dioxide, which is quartz, for our chip. Considering the advantages and disadvantages of various approaches taken by researchers preceding us, we decided to use thermally oxidized intrinsic silicon wafer for fabricating our chip. Using intrinsic silicon ensures that there are minimum amount of stray carriers in the bulk of the material, thus reducing the problems caused by capacitance from the chip. Thermal oxide of intrinsic silicon leads to undoped quartz. Oxidized silicon wafers are readily available.

Given the dimensions of most mammalian cells, a 50-60 μm transparent window is necessary in order to properly observe the cells with the optical microscope and based on these dimensions and strength of thermally grown silicon dioxide, we estimated that a 1 μm thick silicon dioxide layer should be sufficient for our chip. These dimensions would also give us capacitance and resistance values that were well within the acceptable range. We determined that double-sided polished 4-inch, 400μm thick (100) silicon wafers (University Wafers) with 1 μm thick thermally grown oxide (Figure 3.3a) would be the ideal working material for micro-fabricating the chip. The bottom-side oxide acts as an insulator for any currents leaking through the silicon layer. Each wafer would have an array of chips (Figure 3.2), each with dimensions of 1 cm x 1 cm with each chip having a single 1.5 μm diameter pore. The excellent optical properties of SiO_2 based patch clamp make it more amenable to integrating with an optical microscope. As illustrated in figure 3.5, the micron-sized aperture for patching the cell is formed in the top silicon dioxide membrane. The relatively large chip size was chosen for the consideration of integrating patch clamp recording with other modes of cell biological studies in the future.

3.2 FABRICATION PROCESS

Even though the sequence of steps in a given process is well established, in order to obtain good tolerance on outcomes, it is important to carefully control parameters in individual step. A typical lithography process involves several steps:

1. Photoresist spin-coating (photoresist dispensing, acceleration, spin speed, time)
2. Pre-bake (temperature, time)
3. UV exposure (dose, time); in case of electron-beam lithography (current, dwell-time, beam speed, area dose)
4. Development (developer concentration, time, temperature)
5. Post-bake (temperature, time)
6. Etching [Wet (concentration, time, temperature); Dry (type of gas, dilution ratio, substrate temperature, time, pressure)]

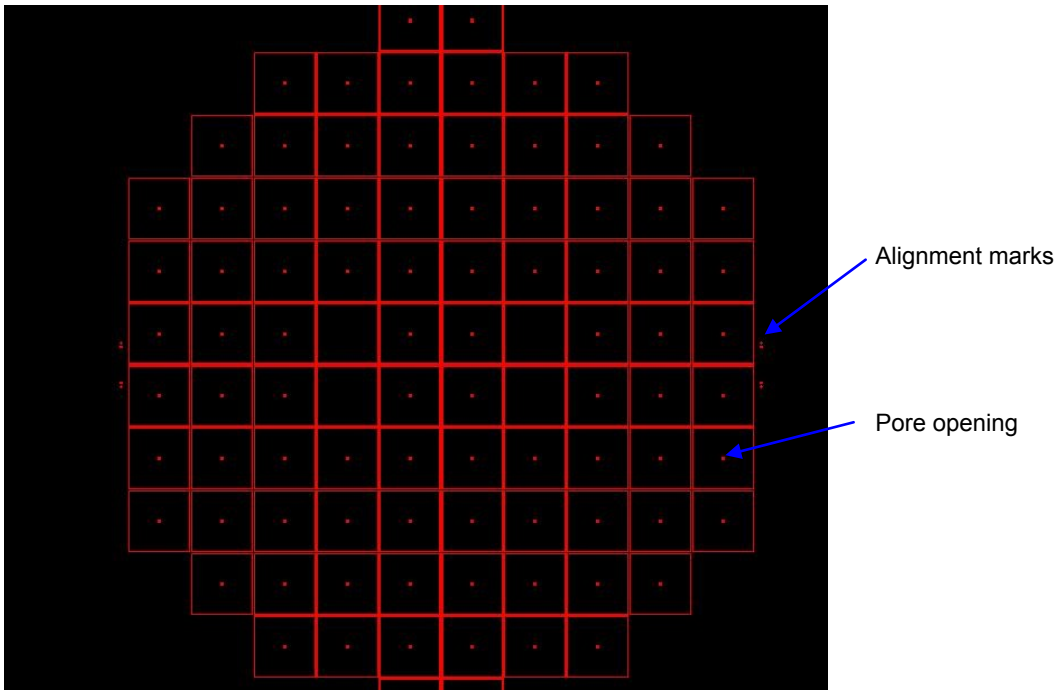

Figure 3.2. AutoCAD snapshot of a sample mask to be used for the back-side photo-lithography step. This defines the 1cm X 1cm array of individual devices (red squares). The small red dots represent the 700 µm square windows for the back-side etching. A 4-inch wafer yields about 92 patch-clamp chips.

The outcome of the lithography process is dependent on careful control of all parameters in these individual steps. Any deviation from the optimized values results in deviation in the dimensions of the desired features. All lithography parameters were optimized (see Appendix A) by carefully varying the process variables of each individual step around the reference values obtained from the datasheets for the chemicals involved. Other microfabrication processes like reactive ion etching, wet etching and XeF_2 etching, etc. were also similarly optimized (see Appendix A).

We tried two different approaches to fabricate the chips:

(i) Wet fabrication process: Apertures with diameter of 0.5 μm were patterned on one side of the wafer (top side for the device) using electron-beam lithography with polymethyl methacrylate (PMMA; Microchem, Corp. Newton, MA) as the electron beam resist and square apertures 700 μm on the side were patterned on the other side and aligned such that the circular apertures on top remains at the center of the square using standard photolithography with a positive photoresist (Shipley Co., Inc. Marlboro, MA) (Figure 3.3c). The silicon dioxide layers from top and bottom were then etched using buffered hydrofluoric acid (BHF; J T Baker Phillipsburg, NJ) solution. After removing the resists in acetone (Sigma-Aldrich, St. Louis, MO) (Figure 3.3d), the silicon substrate was etched using 5% tetramethyl ammonium hydroxide (TMAH; J T Baker), an anisotropic etchant for silicon, at 90 ^{o}C (Figure 3.3e). The process formed a ~2 μm diameter pore in the top silicon dioxide membrane[1]. TMAH has a very high etch rate along the <100> and <110> directions of silicon compared to that along the <111> direction. This resulted in a signature pyramidal pit as silicon is etched by TMAH. Because of this etch-

[1] The lateral etch rate of silicon dioxide in buffered HF is found to be ~0.7 times that of vertical etch rate, most probably due to dimensional constraints.

rate difference, the 700 μm on the back face of the wafer will be narrowed to about 75 μm. TMAH etch rate for silicon dioxide is negligible and leaves the top oxide thickness unchanged.

(ii) Dry Process: Apertures with diameter of 1 μm were patterned on one side of the wafer (top side for the device) using electron-beam lithography with polymethyl methacrylate (PMMA; Microchem, Corp. Newton, MA) as the electron beam resist and circular apertures 75 μm in diameter were patterned on the other side, aligned to the circular apertures on top, using standard photolithography with a positive photoresist (Shipley Co., Inc. Marlboro, MA). The silicon dioxide layers from top and bottom were then etched using reactive ion etching (RIE) (Trion Technology, Clearwater, FL). After removing the resists in acetone (the cross-section looks similar to the one in Figure 3.3d), the silicon substrate was etched using xenon difluoride (XeF_2) isotropic dry etching technique (Xactix, Inc., Pittsburgh, PA). The dry process formed a 1 μm sized pore in the top silicon dioxide membrane with a window size of 75 μm in diameter, while the opening on the bottom side was about 875 μm because of isotropic etching of silicon.

We concluded that the dry process was more reproducible and provided better pores with a flat profile. This resulted in higher success rate in obtaining good seals while patching the cells. The dry process was, therefore, used for the final mass production of the patch clamp chips.

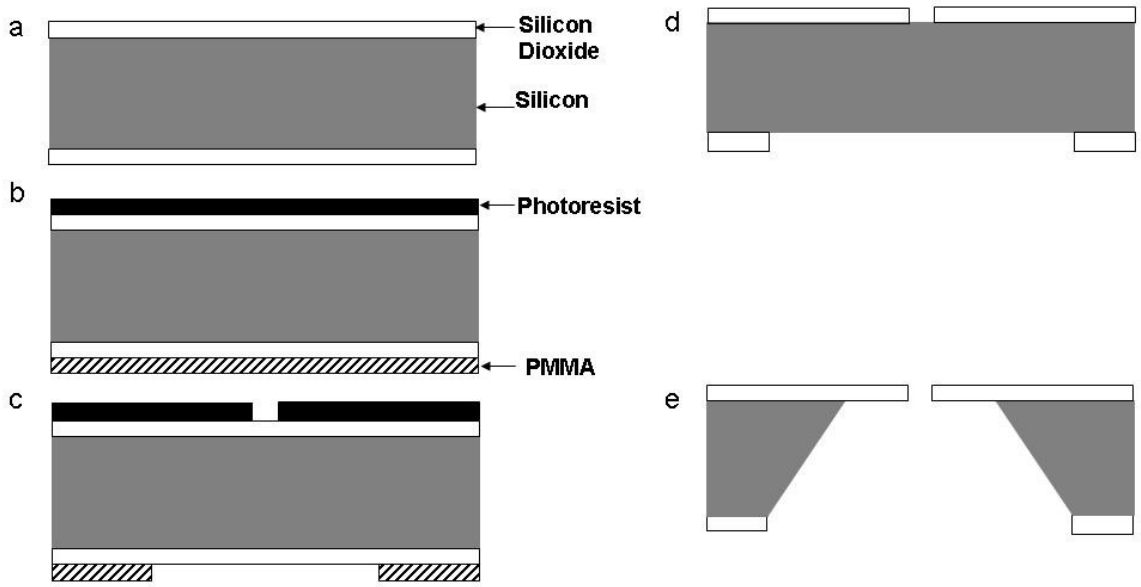

Figure 3.3. Schematic for fabrication of the chip (not to scale): (a) Oxidized silicon wafer was used as the starting material. (b)PMMA and photoresist were spin-coated on the top and the bottom respectively. (c) 0.5µm circles were defined in PMMA using electron beam lithography and squares of about 650µm were defined, aligned to the top circles from the back of the wafer in the photoresist using photolithography. (d) Silicon dioxide was isotropically etched using buffered hydrofluoric acid (BHF); PMMA and photoresist were then removed. (e) Silicon was etched anisotropically using TMAH.

All fabrication was performed using the equipment available at the NanoScale Fabrication and Characterization Facility of the Petersen Institute of NanoScience and Engineering on the University campus. We used the spinner for coating photo- and electron-beam resists, the mask-aligner for photolithography, the electron-beam lithography system, the reactive ion etching system, and wet-chemical benches for etching and cleaning the wafers. We used the scanning electron microscope facility at the University's Center for Biological Imaging was used to characterize the pores. Optical microscopy and electrical characterization (with a patch clamp amplifier) was performed using our in-house equipment.

3.3 MICROFLUIDICS: DESIGN AND FABRICATION

In order to bridge the gap in understanding of MS channels, it is necessary to avoid confounding factors from indirect stimuli like changes in intracellular processes and stress distributions over a large area, and perform electrophysiological studies under direct mechanical stimulus. Chip-based planar patch clamp approach has the potential to provide a stable platform for electrophysiology with direct mechanical stimulus using equipment such as an atomic force microscope. Our objective was to integrate chip-based planar patch clamp assembly with an atomic force microscope (AFM) and an optical microscope while providing a perfusion chamber for exchange of physiological buffers necessary for biological experiments. To attain this objective, we designed a microfluidic liquid cell to provide sufficient access for an AFM cantilever from top side of the chip while keeping the chambers thin enough to allow for a long working distance high magnification lens of an inverted optical microscope from the bottom side. This would allow us to simultaneously combine electrophysiology with high-resolution optical microscopy and atomic force microscopy.

In order to perform high quality whole-cell electrical recordings, we needed to electrically isolate the top and bottom sides of the chip to minimize the current leaking between the intracellular and extracellular solutions. This required a liquid cell that can house the chip such that the top and bottom sides of the chips are impermeable to any liquid on either side of the chip, and that the material of the liquid cell be an insulator. The liquid cell also needed to provide

space for Ag/AgCl electrodes on top and bottom to apply the voltage and record the current. The electrical separation of the top and bottom sides of the chip was achieved with an O-ring on the bottom side of the chip. Our theoretical calculations suggest that depending on the temperature and the precise contents of the buffer being used, our chip (with a 1μm deep pore with a diameter of 1μm) would have resistance on the order of a few hundred kilo-ohms.

The dimensional constraints for the liquid cell were governed by the working distance of the microscope's objective lenses (the longest working distance objective available to us is 60x with 1.3 mm working distance) as well as to allow contact between the cell and the AFM cantilever. The goal of our design was to leave the top of the chip uncluttered while making the bottom of the liquid cell thin and transparent. Furthermore, the design required space for electrodes. Given the design of the cantilever holder for our AFM (MFP-3D by Asylum Research, Santa Barbara, CA), the closest clasp for the chip on top needed to be less than 400 μm thick while being at least 6 mm away from the center of the chip. In order to visualize the cell using our optical inverted compound microscope (IX71 by Olympus, Center Valley, PA) at sufficiently high magnification, the thickness of the bottom side chamber of the liquid cell needs to be less than 500 μm to incorporate the 402 μm thickness of the chip. The chamber was designed to seat the chip on a small circular reservoir, 8 mm in diameter and 0.4 mm deep, with three feed lines (1 mm in diameter) coming into it. Two of the feed lines serve to exchange the intracellular buffer and the third to hold the recording electrode. The assembly had another piece that pressed on the chip from top and had another O-ring and three feed lines similar to the ones on the bottom side built into it (Figure 3.4). The ultra thin rubber O-rings for the assembly were obtained from Apple Rubber Products, Inc. (Lancaster, NY). The electrode on the top side acted

as the extra-cellular ground electrode and the electrode in the bottom reservoir served as the intra-cellular recording electrode.

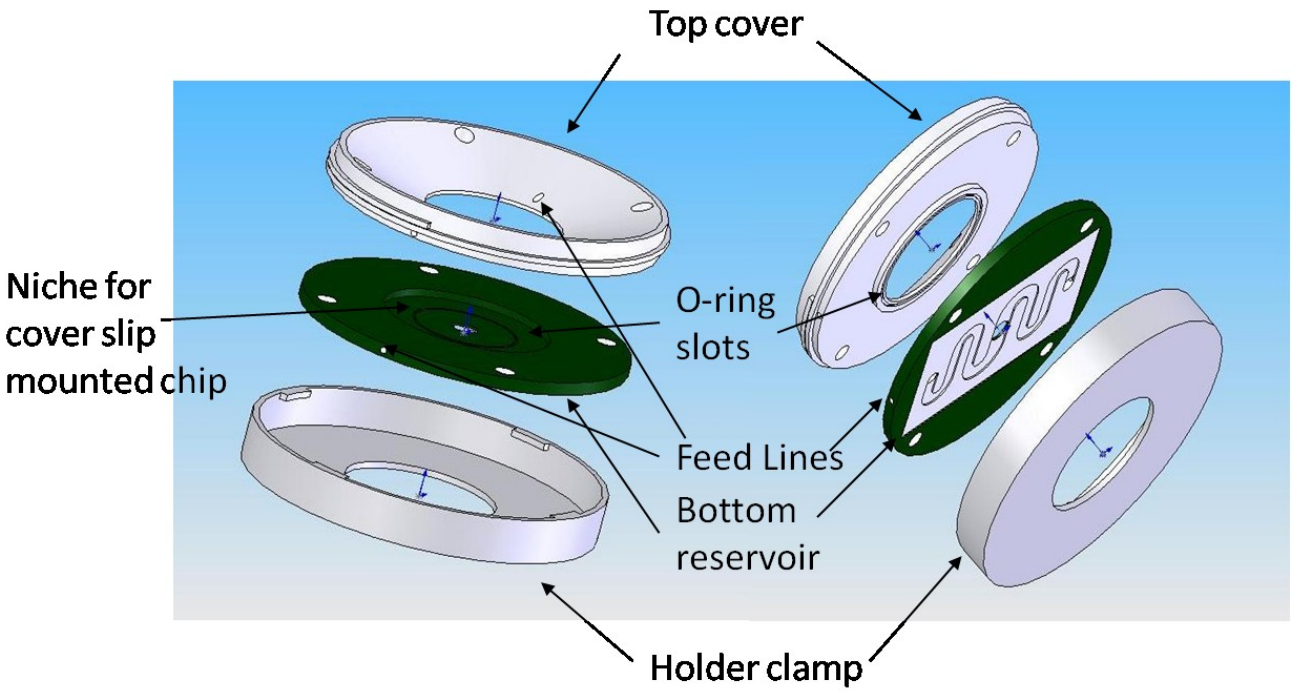

Figure 3.4. Design of the liquid cell.

The chamber was designed using the 3-D modeling software SolidWorks (Dassault Systèmes SolidWorks Corp., Vélizy, France) and fabricated using 3D stereolithography. We used the photopolymer called WaterShed XC 11122 by DSM Somos (Elgin, IL), because of its low viscosity (for the high resolution we need), high transparency (RI: 1.15) and suitable mechanical properties (WaterShed XC datasheet).

4.0 CHARACTERIZATION OF THE PLANAR PATCH CLAMP CHIP

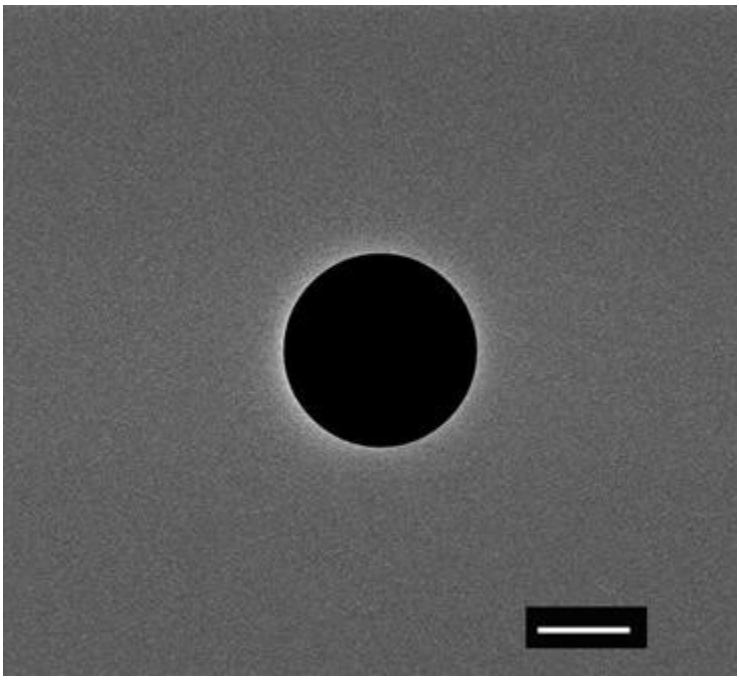

Figure 4.1. Scanning electron micrograph of the pore in a sample, representative chip. The scale bar at the bottom is 0.5 µm.

We characterized these chips using optical microscope for obvious flaws and scanning electron microscope (SEM) for a closer observation. Since MEMS fabrication techniques are known to provide consistent fabrication and SEM imaging is time intensive, we sampled a few chips for SEM observation and found that the fabricated pores in the silicon dioxide membrane had consistent geometries (Figures 4.1 and 4.2).

The ultimate test of the chip and the liquid cell is the success rate with which we can perform whole cell patch clamp experiments. Pheochromocytoma (PC12) and Chinese hamster ovarian (CHO) cells were used for proof-of-concept whole-cell-patch experiments, while also testing for possible giga-ohm seal to determine whether we can perform single-channel experiments with this apparatus. Literature suggested that the success rate for obtaining good whole-cell recordings from chip based systems is not more than 25-30% (Sigworth and Klemic 2005). This gave us an opportunity to test whether our design is at par with the existing designs in terms of the success rate; we performed recordings with both PC12 as well as CHO cells to estimate our rate of success.

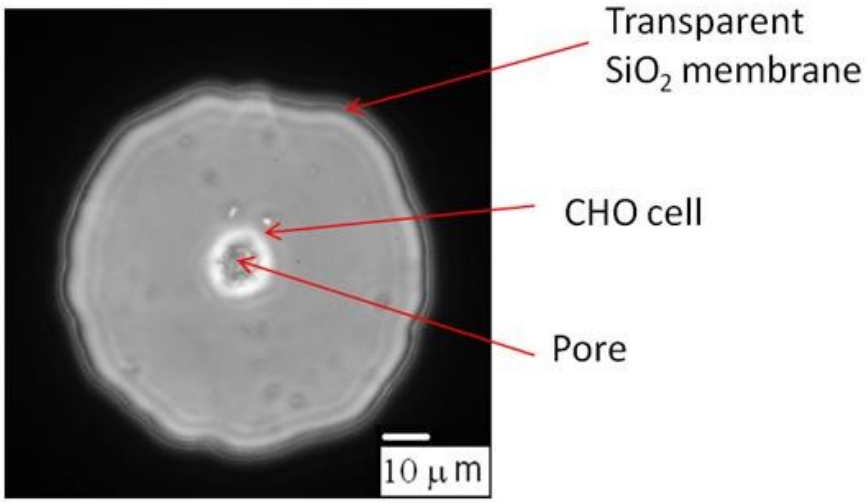

Figure 4.2. A phase contrast optical microscopy image of a CHO cell sitting over the central pore on the circular SiO_2 membrane window. The dark, opaque portion surrounding the membrane is the silicon as seen from the bottom of the chip.

Open-pore resistance – resistance between the top and bottom electrodes with the respective buffers present but not the cell – was used as a criterion for characterizing the quality of the chip. The open-pore resistance is proportional to the depth of the pore and inversely proportional to the square of its radius. Depending on the temperature and the precise contents of the buffer being used, a 1μm deep pore with a diameter of 1μm would have resistance on the order of several hundred kilo-ohms. We built an open top aluminum box to use as a Faraday Cage to isolate the patch clamp measurements from ambient electromagnetic radiation. The box was placed upside down on the microscope stage when electrical recordings were being performed.

It was necessary to discard some chips for quality control. Chips with open-pore resistances of 2 MΩ or higher were discarded. Chips showing resistances <100 MΩ in cell-attached configuration, measured using PC12 and CHO cells, were also discarded. The distribution of seal resistance for 57 chips (with >100 MΩ seal resistance) is shown in figure 4.3. From the sample of chips, seal resistances of >1GΩ were achieved in 8 instances with the maximum seal resistance being 1.22 GΩ. It was observed that chips having higher open-pore resistance usually yielded higher seal resistance. A typical current trace during the process of formation of a whole-cell patch is shown in figure 4.4.

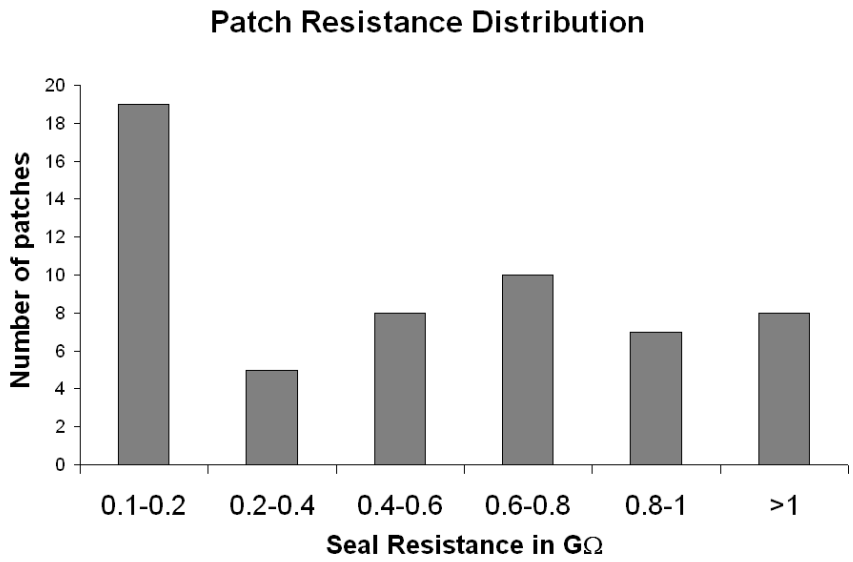

Figure 4.3. Distribution of seal resistance: seal resistance in cell-attached configuration for CHO and PC12 cells using 57 different chips.

4.1.1 Electrophysiology using planar patch clamp chip

Chinese Hamster Ovary (CHO), pheochromocytoma (PC12) and human keratinocytes (HaCaT) were used to study the characteristics of our device. All cells were cultured at 37 ^{o}C with 5% ambient CO_2 in 76 mm culture dishes. CHO cells were grown in F12 media (Sigma-Aldrich, St. Louis, MO) with 10% fetal bovine serum (FBS) and 1% (v/v) antibiotic-antimycotic solution (10 mg/ml Penicillin, 10 mg/ml Streptomycin and 25µg/ml Amphotericin B; Mediatech, Inc., Manassas, VA). PC12 cells were grown in DMEM media (Sigma-Aldrich) with 5% FBS and 1% antibiotic-antimycotic solution.

An important pre-requisite for good quality electrical recordings is that the media containing target cells be free of any solid non-cellular material which could potentially fully or

partially clog the pore and impair the formation of a good seal. In order to achieve this, we developed a simple protocol to extract cells from the culture (see Appendix B). Briefly, we aspirate the culture medium from the dish and after rinsing the cells 3 times with phosphate buffered saline (PBS). We add 3 ml of 0.25% trypsin-EDTA solution and incubate the cells at 37^{o}C for 5 minutes. After gentle agitation, the trypsin-EDTA solution is aspirated out into a centrifuge tube and 3 ml of culture medium is added to the tube to inhibit trypsin activity. The culture dish is refilled with 10 ml of culture medium and replaced in the incubator. The tube with cells is centrifuged at 10,000 rpm for 4 minutes and the supernatant is removed and discarded. After adding 3 ml of PBS to the cellular pellet remaining behind in the tube, the trypsin treatment is repeated to ensure that all the extra-cellular debris is hydrolyzed. A small amount of the suspension is observed under a phase-contrast microscope to check for debris. Trypsin treatment is repeated for smaller amounts of time until no debris are seen in the suspension. The shorter subsequent trypsin treatments (if necessary) ensure that the extracellular domains of membrane proteins remain unaffected by trypsin. Finally, the cells are suspended in isotonic extra-cellular buffer necessary with sufficient dilution for the specific experiment.

For whole-cell recordings, we used a commercially available patch-clamp amplifier (model 2400, A-M Systems, Carlsborg, WA) and the shareware electrophysiology data acquisition software (WinWCP v3.5.6, Strathclyde Electrophysiology Software, Strathclyde Institute of Pharmacy and Biomedical Sciences, University of Strathclyde, UK) on a standard PC (Dell, Inc., Round Rock, TX) with National Instruments (Austin, TX) PCI-6070E multifunction data acquisition card. The data was sampled at 10 kHz and filtered at 2 kHz. All the data acquired was archived to the hard-drive of the PC. The intracellular buffer (on the bottom side of

the chip) used for the electrical recordings consisted of 125 mM KCl, 2 mM $CaCl_2$, 1 mM $MgCl_2$, 10 mM EGTA and 5mM HEPES. The final free Ca^{2+} concentration was ~ 1 μM at a pH of 7.4. Basal Media Eagle's (Sigma-Aldrich) without the pH indicator was used as extracellular buffer (on the top side of the chip). The same buffers were used for all of cells unless specifically stated otherwise (see Appendix D for buffer recipes). The chip was used as a replacement for the micropipette to perform the patch-clamp experiments. Ag/AgCl electrodes from the top and bottom sides of the perfusion chamber were connected to the patch-clamp amplifier.

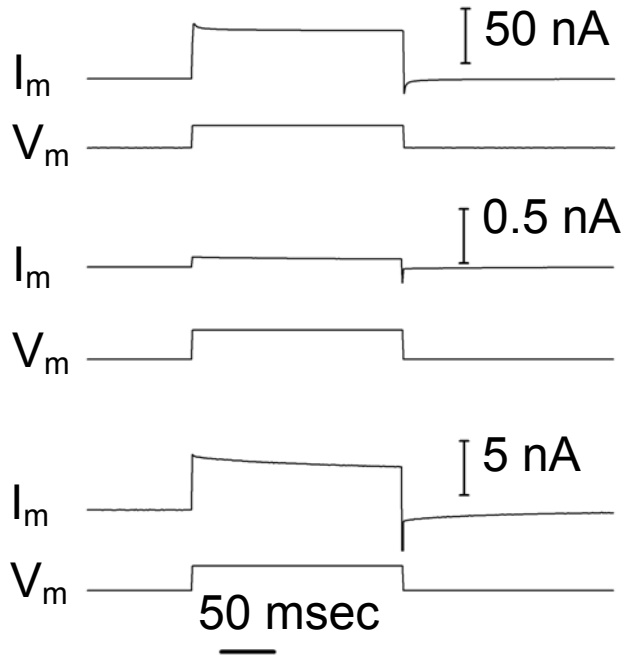

Figure 4.4. Current (I_m) responses to a 100 mV voltage step (V_m) for: (top) an open pore, (middle) cell plasma membrane forming giga-ohm seal, and (bottom) a whole-cell patch clamp of a CHO cell.

The simplicity of our device stems from the ease of use during the patching process. The bottom reservoir of the perfusion chamber was filled with the intra-cellular solution while ensuring that there were no air-bubbles, the chip was placed on the reservoir after wetting the

pore properly and the top half of the chamber was fixed on to seal the chip. The cell suspension was then added to the top side of the chip. Figure 4.2 shows a typical chip with a cell observed from the bottom side of the chamber. While the cells settle for about 30 seconds, gentle positive pressure was applied from the bottom side to keep any possible small particle contaminants away from the pore. The pressure was the switched to a gentle suction to draw the cell to the pore. The resistance across the pore was simultaneously monitored. The suction was stopped after the resistance saturated (leading to what is called a cell-attached configuration) to a high value (100s of MΩ to GΩ) and a sharp, more intense suction pulse was applied from the bottom side to rupture the patch of the cell's plasma membrane sealed in the pore, thus giving access to the inside of the cell and forming a whole-cell patch. Pressures were applied or changed manually using a syringe. The entire patch clamp process takes less than two minutes. While a microscope is not needed during the process, the perfusion chamber design allows imaging by an inverted, reflecting optical microscope from the bottom-side (see Appendix B for the protocol).

The efficacy of the chip is determined by how well we can record whole-cell currents from cells. In order to test this, we used both CHO and PC12 cells to perform whole-cell recordings. We were able to successfully record whole-cell currents from CHO (n=9) and PC12 (n=16) cells choosing from chips which provided >600 MΩ seal resistance. Instances with seal resistance <600 MΩ were deemed to be too leaky and no whole-cell recording was attempted. The cell membrane potential was clamped at -70 mV (which is sufficiently close to the resting potential) for both types of cells. Typical current response to step changes in the holding potential of a CHO cell is shown in figure 4.5a. The whole-cell I-V relationship for CHO cells is shown in figure 4.5b and for PC12 cells is shown in figure 4.6. Our results are in agreement with

previous measurements using conventional pipette based patch clamp found in the literature (Dichter, Tischler et al. 1977; Janigro, Maccaferri et al. 1989; Gamper, Stockand et al. 2005).

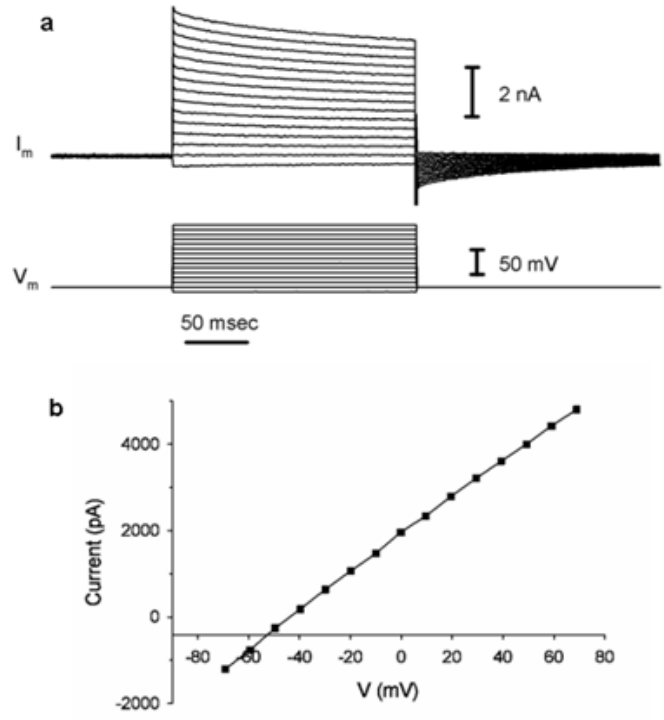

Figure 4.5. (a) Representative current responses of a CHO cell to step changes of holding potential in whole-cell configuration. (b) I-V relationship of a CHO cell in whole-cell configuration.

PC12 cells were used to perform potassium blocking and recovery experiments by adding Ba^{2+}, a selective and reversible blocker of certain types of K^+ channels (Armstrong, Swenson et al. 1982) to the extra-cellular solution. Since PC12 cells express several types K^+ channels (Hoshi and Aldrich 1988), we expected to see a drop in outward current after the introduction of barium chloride in the extra-cellular solution. Figure 4.6 shows the I-V relationship of a PC12 cell in whole-cell configuration before (squares) and after (solid circles) the addition of 1 mM $BaCl_2$ to the extracellular solution. The Ba^{2+}-sensitive current is plotted in the inset. The reversal

potential of the Ba^{2+}-sensitive current is ~ -72 mV, which is close to the K^+ equilibrium potential under our experimental conditions (the experimental Nernst potential $E_K = \frac{RT}{F} \ln \frac{[K^+]_{out}}{[K^+]_{in}} \approx -81$ mV, $[K^+]_{out}$ = 5.3 mM, $[K^+]_{in}$ = 125 mM, and T = 25 ºC, R and F are gas constant and Faraday constant respectively). The difference between the calculated and measured reversal potential is attributed to the presence of Ba^{2+} insensitive K^+ channels present in PC12 cells as well as to the leak current from the cells.

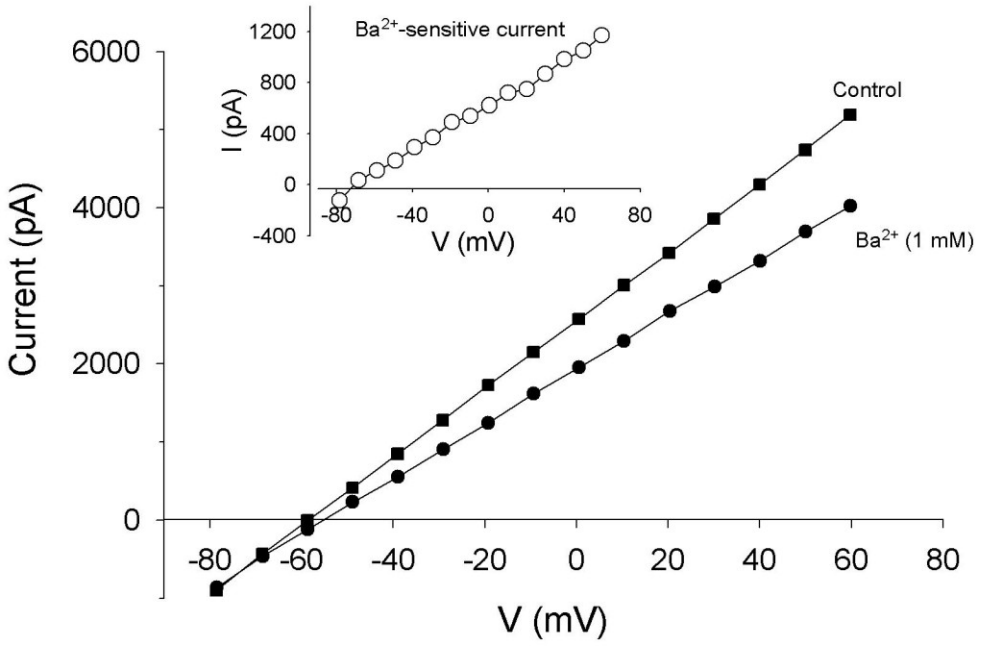

Figure 4.6. I-V relationship of a PC12 cell in whole-cell configuration under normal conditions (squares) and after addition of 1 mM $BaCl_2$ (solid circles). Inset: I-V relationship for the Ba^{2+}-sensitive current (the difference between current in the absence and the presence of Ba^{2+}) (open circles). The reversal potential of the Ba^{2+}-sensitive current is ~ 72 mV, very close to the experimental equilibrium potential of K^+.

As a demonstration of our ability to perfuse the intra-cellular buffer to add pharmacological agents of interest, we perfused amphotericin B into the bottom-side reservoir of

the chamber. Amphotericin B is known to form large non-selective cation channels in cell membrane (Rae, Cooper et al. 1991). Formation of these large non-selective cation channels in the patch of membrane covering the pore in the cell-attached configuration should result in the so-called perforated patch. Higher resistance than offered by the cell in the whole-cell configuration is expected in the perforated patch configuration. To test this we applied step-wise increasing voltage pulses to a CHO cell in cell-attached configuration 5 minutes after perfusing amphotericin B (200 µg/ml) and the current response was recorded. The current response to voltage pulses is shown in figure 4.7. One can clearly see that the resistance offered by the cell is higher (about 18 MΩ) than what is observed in the whole-cell configuration (about 5-6 MΩ) (fig. 4.5a).

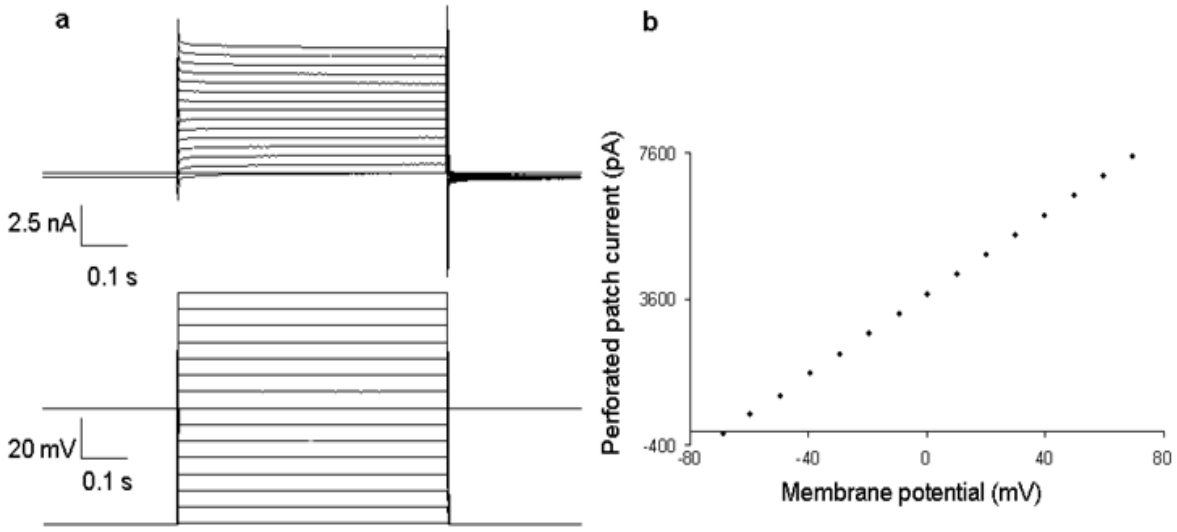

Figure 4.7. Current response of a CHO cell in perforated patch configuration: (a) Response to voltage pulses of different magnitude. (b) I-V relationship 5 minutes after introduction of amphotericin B in the intra-cellular solution in cell-attached configuration. The I-V curve for CHO cell before introducing amphotericin B is seen in Fig. 4.5b.

In summary, we designed and fabricated a planar patch clamp chip capable of forming giga-ohm seals with a success rate comparable to other available techniques including conventional micropipette based patch clamp. Our perfusion chamber assembly allows for the exchange of extra-cellular as well as intra-cellular buffers making possible a wider range of pharmacological experiments to be performed using this apparatus. Since the assembly is not sensitive to vibrations the total amount of recording time available for each patched cell has been significantly improved.

5.0 WHOLE-CELL ELECTRICAL RESPONSE TO DIRECT MECHANICAL STIMULUS

Having tested our planar patch clamp chip for whole-cell recordings, we wanted to study the current response of cells to a direct mechanical stimulus by integrating our planar patch clamp system with an atomic force microscope (AFM). We used the AFM in our lab (MFP-3D, Asylum Research, Santa Barbara, CA) to perform this set of experiments using HaCaT cells as the model system, since HaCaT cells, unlike PC12 and CHO cells, are known to express MS channels. The AFM head was mounted on the stage of an inverted compound optical microscope (IX71, Olympus, Center Valley, PA). The perfusion chamber and chip assembly was placed on the microscope stage with appropriate buffers (figure 5.1).

HaCaT cells were grown in DMEM media with 10% FBS and 1% antibiotic-antimycotic solution. The cells were isolated using the protocol detailed in Chapter 4 above (also see Appendix B). About 500 µl of the cell suspension was placed on the top side of the chip and cell was patched using the protocol described in Chapter 4 (also see Appendix B). The AFM head was then placed on top of the chamber and the cantilever aligned over the patched cell. This was achieved by moving the stage while observing the cell with the microscope. Once the cell and the cantilever are aligned, we used the AFM control software to indent the patched HaCaT cell while simultaneously recording the whole cell current through the cell. Indentations were

performed at a rate of 4 Hz. Deflection data from the AFM was collected by a data acquisition card (National Instruments, Corp., Austin, TX) simultaneously with the data from the patch-amplifier, and stored on a computer. Patched cells could be held at a variety of voltages depending on the experiment. We used long, thin, triangular silicon nitride cantilevers with pyramidal tips and a nominal spring constant of about 0.1 N/m for these experiments.

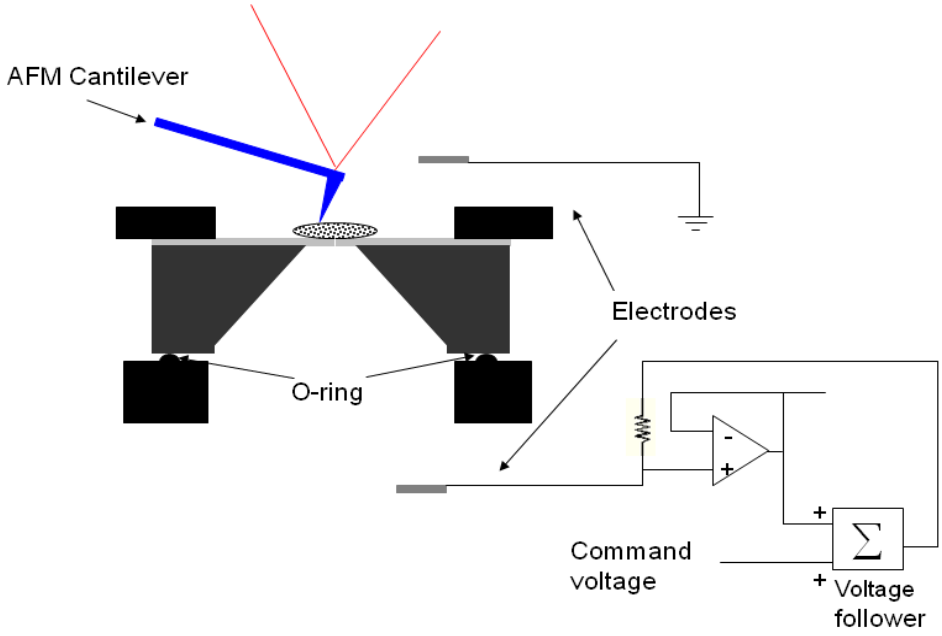

Figure 5.1. Schematic of the planar patch clamp assembly integrated with an AFM.

The deflection of the AFM cantilever off the cell surface provides a mechanical stimulus and the resulting current from the MS channels produces a highly repeatable waveform. The peculiar shape representing each indentation (figure. 5.2) is the result of the cantilever dynamics while indenting the cell. As the cantilever approaches the cell from a distance and makes contact with the cell and makes an indentation, it bends upwards represented by the negative spike. The

small upward deflection at the tail end of the photodiode voltage curve is caused by the cantilever "sticking" to the cell.

To characterize the contact geometry and timing of channel dynamics we define several kinetic parameters for the current response in the representation photodiode voltage corresponding to high resolution view of the current response from a single indentation (figure 5.2):

- t(indent) - time over which cantilever is in contact with the cell membrane;
- t(1/2) – time between onset of current and current peak value;
- t(peak_lag) – time between the max indentation depth and current peak;
- t(delay) – time between membrane contact and onset of current;
- t(open) – time over which the channels are open.

The parameter t(indent) is obtained from the AFM control circuit whereas the rest of the parameters are obtained from the electrophysiology measurements.

In the simplest model of stress caused by cantilever indentation, the cantilever indents the cell membrane, the lipid bilayer in the immediate vicinity of the point of indentation is compressed which causes stretching of the lipid bilayer further away (figure 5.3) up to a certain distance creating a stress field. As the depth of indentation is increased, the radius of the stress field also increases until the flexibility of the bilayer membrane itself dissipates the stress at a saturation indentation depth. Some of the stress energy might also be dissipated as the MS channels within this radius are activated. Beyond this distance, the amount of stress is not

sufficient to provide the required energy to induce conformal changes in the ion channels. Thus, each indentation is capable of providing sufficient energy to activate several ion channels within the stress field, resulting in a current response that is dependent on the local channel distribution.

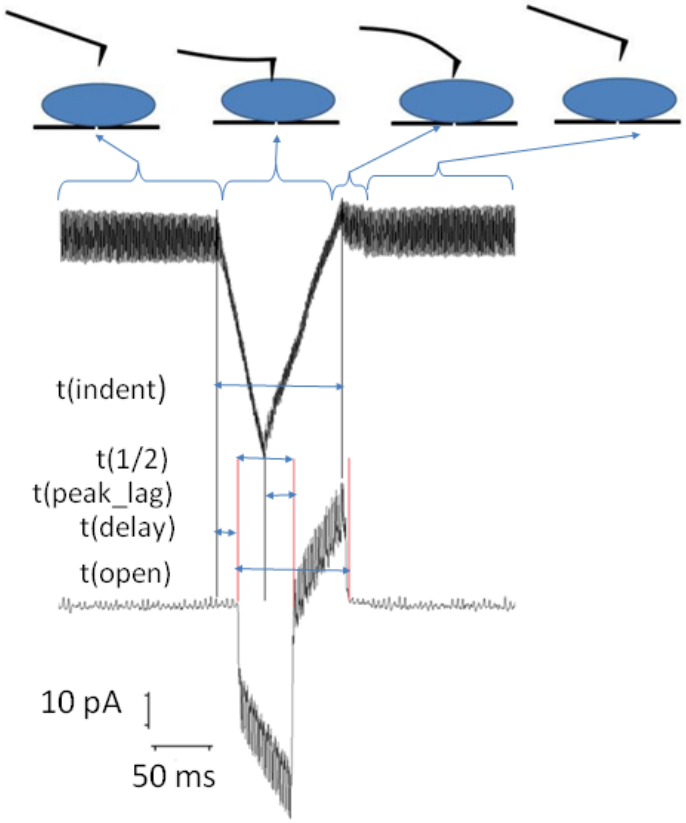

Figure 5.2. Cantilever indenting a voltage clamped cell. Cartoon depiction (top) of various stages of the indentation process as manifested in voltage output from the photodiode (upper trace) and the corresponding whole-cell current in response to an indentation (lower trace). Kinetic parameters pertaining to the process are indicated.

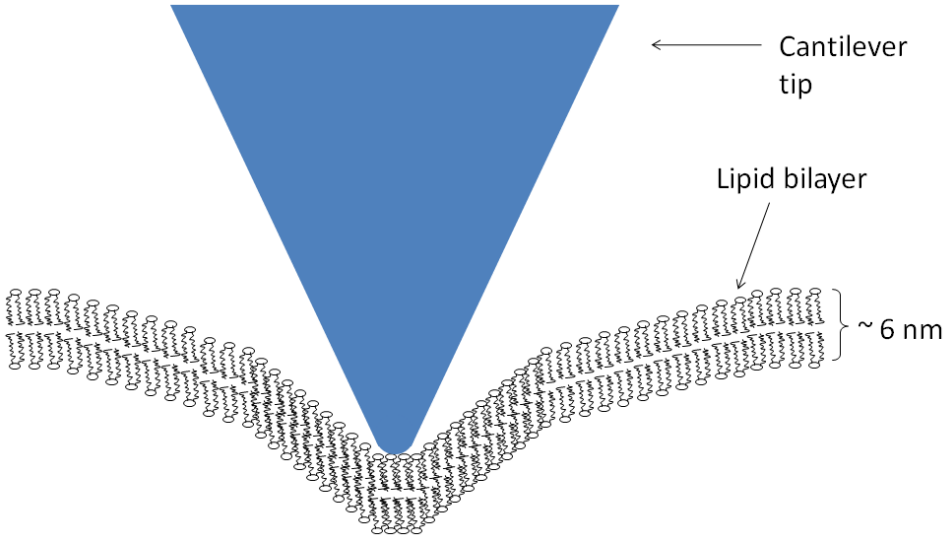

Figure 5.3. Cartoon showing the effect of cantilever indentation on the cell membrane. As the cantilever indents the cell membrane, the lipid bilayer in the immediate vicinity is compressed resulting in stretching of the lipid bilayer away from the cantilever. This stretching effect is for a limited distance as the stress is dissipated because of the fluidity of the bilayer membrane and the presence of large amounts of excess bilayer. Literature suggests that a sharp cantilever can indent the bilayer for up to 45 nm before it is ruptured.

5.1 MAPPING CHANNEL DISTRIBUTION

The distribution of MS channels across the cell membrane is unknown. The probability of getting a current response from an indentation at any given spot is, therefore, unknown. Why and how this current response varies spatially may provide valuable clues towards mechanisms of mechanosensation and could be relevant to models of mechanosensitivity in ion channels. To address this question, we performed an array of indentations over a 5 μm x 5 μm area on HaCaT cells which are known to express TRPV4 amongst other MS channels. In order to ensure that the

current through MS channels is solely because of the chemical potential of the respective ions, the cells were voltage clamped at 0 mV.

We used long, thin, triangular silicon nitride cantilevers with pyramidal tips and a nominal spring constant of about 0.1 N/m for these experiments. Previous studies (Obataya, Nakamura et al. 2005; Kwon 2009) suggest that for sharp, thin cantilevers, depending on the specific cell type, the cell could be indented for depths of up to 50 nm before the lipid bilayer ruptures. Visual analysis of the force curves obtained from HaCaT cells for various indentation depths indicated that there were no bilayer rupture events for indentation depths of up to 45 nm. Given the cantilever parameters, fluidity of the lipid bilayer (Evans and Needham 1986; Dieluweit, Csiszar et al. 2010) and the presence of large amount of excess membrane, we estimate that an area of not more than 250 nm in radius is affected by each indentation, even for indentations as deep as 45 nm. Hence, a 10 x 10 array was chosen for the area to keep two consecutive indentation points 500 nm apart, sufficiently long to avoid overlap of area affected by neighboring indentations. We chose an indentation depth of 25 nm for these experiments to make sure that no bilayer rupture events occur during the mapping process. With this protocol we mapped the distribution of MS channels by recording currents at each indentation point.

The current values obtained from indenting the 10 x 10 grid (over a 5 μm x 5 μm area) on the cell are represented in grey-scale (large current indicated by white and low current indicated by black pixels; figure 5.4a). Each indentation is represented by the voltage measured across the photodiode as the cantilever deflects while indenting the cell. Repeating the mapping of the same

area under different conditions takes about 5 minutes, including the time needed to exchange the solutions and adding requisite chemical agents.

From the current response (labeled HaCaT in figure 5.4a), it is apparent that MS channels are not uniformly distributed over the cellular surface of HaCaT cells, and that the current is inward and varies for consecutive indentations. We attribute this inward current to calcium flowing into the cell through mechanosensitive channels (most likely TRPV4) present on the HaCaT cells that are activated by mechanical stimulus provided by the AFM cantilever. In order to test this hypothesis, we added 1mM Gd^{3+} (a known blocker for calcium conducting mechanosensitive channels) to the extra-cellular solution and found that the current response seen in HaCaT cells is eliminated. As a control, we repeated the experiment with CHO cells as and indentations do not induce any response from CHO cells (figure 5.4b). Using calcium-free extracellular media results in a response similar to CHO cells (labeled Ca-free in figure 5.4).

The maximum current from a single indentation was found to be about 70 pA. For the BME media we used for these experiments the free extracellular calcium concentration is ~1 μm and assuming an intracellular free calcium concentration of ~ 1 nm, the reversal potential for calcium is ~ +90 mV. Average single channel conductance of about 60 pS (Nilius, Vriens et al. 2004)), we estimate that these MS channels are present in clusters and one indentation can activate about 14 or less channels for one indentation depending on the site of indentation.

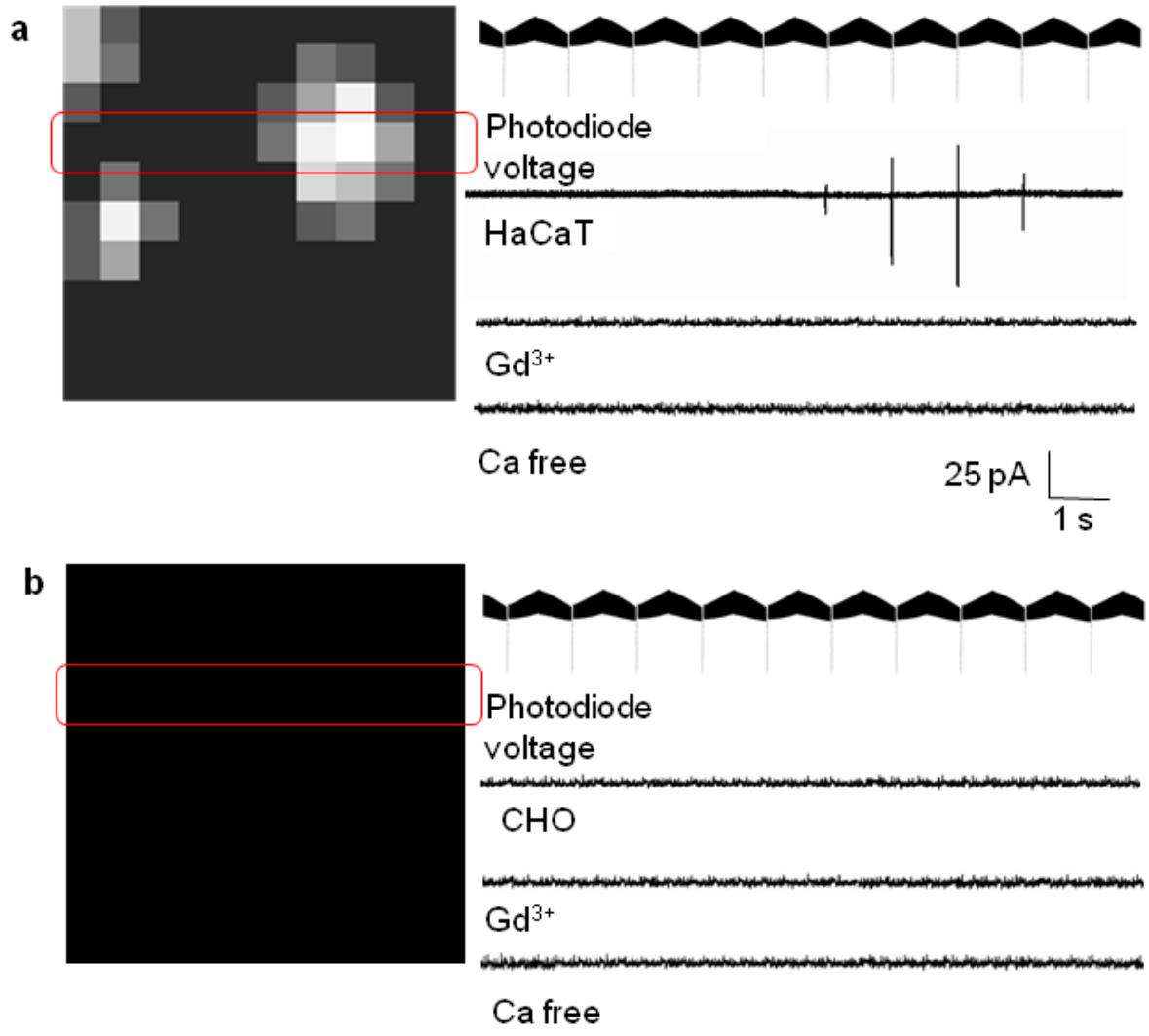

Figure 5.4. Current map in response to indentation by an AFM cantilever. (a) HaCaT cell; (b) CHO cell. Left: representative current response to 10 x 10 grid of indentations over a 5 µm x 5 µm area. Right: voltage output from the AFM photodiode representing cantilever deflection, followed by current response from the highlighted row, followed by the current response from the same row after addition of $GdCl_3$, followed by the current response with calcium free extracellular buffer. There is an approximately 5 minute time difference between each trace with differing conditions.

5.2 KINETICS OF MECHANOSENSITIVE CURRENT

Kinetic parameters, such as time to response, are necessary to construct models of mechanosensation in MS channels. In order to obtain these parameters we positioned the cantilever at the point with highest current and performed multiple indentations (n = 100) at the same spot after the distribution of MS channels was mapped on a section of cell. The data in this experiment was collected at a sampling rate of 100 kHz. This allowed us to compare variation between successive indentations at the same spot as well as cell-to-cell variation (amongst n = 7 cells) at a very high temporal resolution. The same cantilever (k = 0.097 N/m, calibrated using thermal fluctuation method) was used for all the experiments to avoid convolution from variation in cantilever geometry. The cells were voltage clamped at 0 mV to reduce any interference from voltage driven current. The indentation depth was fixed at 25 nm; sufficiently high without causing membrane rupture events. We have defined some of the important kinetic parameters in the previous section (see figure 5.2 for the graphic representation).

One of the important parameters that determine the current response is the total amount of time for which the cantilever is in contact with the cell membrane. This parameter (defined in the previous section), t(indent), is dependent on the indentation frequency and rate of indentation, and is, therefore, a controllable parameter. Based on previous reports on TRPV4 channel dynamics, (Nilius, Vriens et al. 2004), we fixed the rate of indentation to allow for t(indent) of about 100 ms. This was deemed sufficiently long for studying activation, possible deactivation of MS channels and other events triggered by MS channel gating. The indentation frequency was fixed at 1 Hz (time between successive indentations 1 s) to allow a long time between successive indentation and avoid effects from saturation/inactivation of the channel.

We find that there is a delay of about 10 ms between the time at which the AFM cantilever contacts the cell membrane and the onset of current. Given the rate of indentation used, this delay may be attributed to a threshold force level necessary for activation of MS channels. The delay of about 22 ms between the time of maximum indentation depth and time of peak current suggests that the MS channels may remain activated for a short duration even after the force is reduced. If we assume that the MS current in HaCaT cells is contributed only by calcium ions, it is possible that calcium-activated potassium channels present on HaCaT cells may be activated because of increased intracellular calcium caused by indentation, explaining the inversion in current beyond the peak.

Table 5.1: Kinetic parameters for current response to indentation in HaCaT cells.

cell no.	t(delay) (ms)		t(peak_lag) (ms)		t(1/2) (ms)		t(open) (ms)	
	avg	sd	Avg	sd	avg	sd	avg	Sd
1	9.82	0.31	22.13	0.37	44.87	0.58	95.61	1.12
2	9.97	0.27	21.96	0.32	45.13	0.63	98.37	1.06
3	10.08	0.26	21.87	0.35	44.92	0.67	97.43	1.16
4	10.11	0.29	22.04	0.31	45.08	0.69	96.89	1.04
5	9.89	0.13	22.19	0.23	44.74	0.55	95.42	1.13
6	9.78	0.33	21.98	0.49	44.47	0.71	96.22	1.23
7	10.02	0.17	21.93	0.26	45.19	0.59	97.49	1.09

There is less than 0.05% variation in response parameters from the same site whereas, about 10% variation between different cells. Although, the variability in the numbers is not surprising, we can learn some important lessons from these values. It is known that the lipid bilayer membrane is fluid and consists of lipid rafts that are mobile. With the rate of indentation, the measurements over on site span about 100 seconds which is considerably long. The small

variation in current values and response parameters for indentations at the same site over such a long period of time indicate that the mobility of MS channel clusters, if any, is very slow.

In summary, multiple indentations at the same spot indicate that channel activity and channel numbers remain stable over a considerably long time intervals and that a threshold force level may be necessary to modulate mechanosensitive ion channels in the immediate vicinity of the indentation site.

5.3 FORCE-CURRENT CHARACTERISTICS

Mechanosensitive channels, by definition, are ion channels that sense and convert mechanical force into ion current. There has been conflicting evidence on the mechanism of force sensing by MS channels and the role of lipid bilayer in activation of MS channels is not completely understood. One of the reasons for our endeavor to integrate AFM with planar patch clamp was to better understand how force on the lipid bilayer is manifested in MS channel activation.

We mapped the MS channel distribution on different HaCaT cells (n = 7) using the same mapping parameters as used in section 5.1 and chose the site with maximum current response on each cell. Each of these sites was indented multiple times (n = 10) with indentation depths of up to 45 nm. For indentations more than 45 nm, membrane rupture was observed. We also varied

the membrane holding potential at each indentation depth to observe the dependence of current voltage (I-V) characteristics of MS channels under mechanical stress. These studies should provide valuable data for modeling the activation/inactivation of MS channels.

We observed that the I-V curve was dependent on the indentation depth (Figure 5.5). A clear threshold is observed (10 nm) below which the MS channels are essentially non-conducting regardless of the membrane potential. Saturation in maximum amount of current is also observed at about 40 nm indentation depth, when increasing indentation depth has no effect on the I-V curve. Between these two indentation depths, we observe that the recorded inward whole-cell current for a fixed indentation depth increases as the membrane potential is made more negative. These observations are generally true for all seven cells. The maximum recorded inward current is about 128 pA at –60 mV for a 40 nm deep indentation. If we make assumptions similar to the mapping experiment (section 5.1), we can conclude that about 24 or less MS channels are activated at an indentation depth of about 45 nm, depending on the exact site of indentation.

From the crude schematic in Figure 5.3, it is easy to visualize that a larger area of the lipid bilayer will be under tension as the indentation depth is increased, thus, recruiting more MS channels. We postulate that the tension in the lipid bilayer produced by indentation depths less than 10 nm may not be sufficient to activate MS channels in the affected area. This would explain the threshold indentation depth for MS channel activation. We think that the low stiffness of the bilayer membrane results in dissipation of tension beyond the area affected by indentation depths of more than 40 nm, resulting in reduced tension in the areas farther off. Any

increase in indentation depth would, therefore, have negligible effect in activating more MS channels, explaining the saturation in recorded currents for indentation depths more than 40 nm.

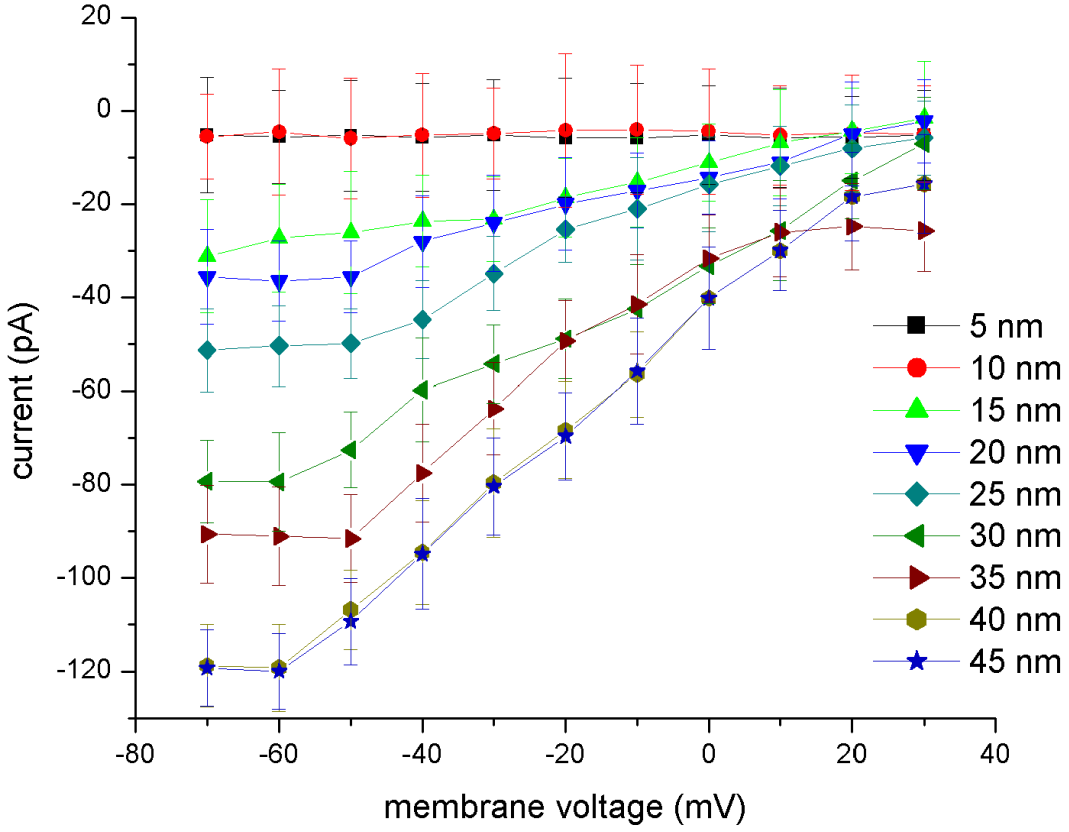

Figure 5.5. Current voltage curves under different force levels (depth of indentation) applied by the AFM cantilever on a HaCaT cell.

6.0 CONCLUSION AND FUTURE RESEARCH

We have designed and fabricated a planar patch clamp chip and allied microfluidics assembly capable of integration with optical and scanning probe microscopy techniques. The patch clamp chip is capable of forming giga-ohm seal with cell-membranes for multiple cell types facilitating whole-cell patch clamp recordings. The microfluidics perfusion chamber for this chip allows for exchange of extra-cellular as well as intra-cellular buffers. We integrate this planar patch clamp chip and the microfluidics with an atomic force microscope to investigate the mechanism of activation in mechanosensitive ion channels using HaCaT cells as the model system. The entire assembly allows us to obtain functional maps of spatial distribution of MS channels across the cell membrane. We also demonstrate the capability of this assembly to perform high resolution kinetic measurements on MS channel activation.

6.1 SUMMARY OF KEY ACHIEVEMETS

We have demonstrated that the silicon dioxide based, microfabricated pores with ~1.5 μm diameter can be successfully used to perform voltage clamp measurements in whole-cell configuration in multiple cell types (CHO, PC12 and HaCaT). The success rate of forming a seal sufficiently good for whole cell recordings (resistance >600 MΩ) was 43% whereas a giga-seal

was achieved in about 15% of the cases. We attribute the low success rate to variation in cellular shapes as well as manual control of applied pressures during the cell clamping process.

The thickness of SiO_2 membrane (1 μm) is sufficient to provide the requisite mechanical strength for the negative pressure impulse needed to rupture the patch membrane covering the pore to go from cell-attached to whole-cell configuration. The planar SiO_2 membrane provides excellent optical transparency and allows optical imaging, including fluorescence microscopy of the patched cell. The top and bottom perfusion chambers allow for rapid solution changes to study the effects of various agonists, antagonists, and other ligands on ion channels. For optical imaging, the SiO_2 membrane is superior to the glass/quartz-based planar patch clamp chip fabricated using the ion-track etching method: the pore inner diameter of the glass chip tapers from ~10 μm on the backside to ~1 μm at the pore opening and the change of glass thickness at the pore opening will induce light interference for optical microscopy imaging of the cell. The architecture of the perfusion chamber allows truly planar whole-cell electrophysiology making the system well suited for multi-modal studies.

We have been able to record from a patched cell for time periods ranging from 35 to 80 minutes. These results are comparable to or better than results obtained from traditional micropipette based and chip based patch clamp recordings. Our assembly is insensitive to mechanical vibrations; vibration isolation of any kind was not necessary.

Integrating the chip and microfluidics with an atomic force microscope gives us a uniquely powerful tool, especially useful for investigating mechanosensitive ion channel

physiology. With this assembly, we have, for the first time, recorded whole cell electrical activity in live HaCaT cells in response to direct mechanical stimulus provided by an AFM cantilever.

We have mapped the distribution of functional MS channels on a live HaCaT cell surface using this assembly. Distribution of various ion channels over the cell surface as well as within the cell has been studied using immuno-staining (fluorescent tags for optical microscopy or heavy metal tags for electron microscopy) (Furness, Karkanevatos et al. 2002). However, a functional mapping of mechanosensitive ion channels in live cells has not been reported.

We observe that MS channels in HaCaT cells are not uniformly distributed over the cell surface. The mechanosensitive current in HaCaT cells is attributed to calcium channels, most likely, conducted through TRPV4 channels. Based on previous studies on TRPV4 channel conductance and our experimental conditions, we postulate that in HaCaT cells, MS channels may be distributed in clusters of up to 25 channels.

We think that the non-uniform distribution of MS channels in HaCaT cells may not be a general feature over all cell types. For cell types with specific mechanical functions, knowledge of MS channel distribution would be key to understanding the physiology of the organ (cochlear cell physiology, for instance) (Langer, Koitschev et al. 2000; Koitschev, Fink et al. 2002). The apparatus can be extended to study the distribution of ligand-gated ion channels by tagging the AFM cantilever tip with various agonists to map the distribution of specific channels.

The high sampling rate measurements possible on our system make it possible to obtain valuable kinetic data on MS channel activation. Automated protocols can indent a specific site with varying rates of indentation and varying indentation depths and record the current at sampling rates of up to 100 kHz. Such high resolution data obtained from recording current response to single indentations by the AFM cantilever tip can be very useful to test models for the structure-function interactions as well as gating dynamics in MS channels.

With our system, we were able to conclude that a threshold indentation depth is necessary to activate MS channels and the flexibility of the lipid bilayer membrane limits the area affected by cantilever indentations deeper than 40 nm.

These results demonstrate the tremendous potential of planar patch clamp assembly integrated with atomic force microscope in performing multi-parametric investigations on MS channels towards better understanding of MS channel physiology.

6.2 FUTURE STUDIES

We have demonstrated that the planar patch clamp chip and microfluidics can be used to perform whole-cell patch clamp recordings with good current resolution. Nevertheless, the success rate for obtaining giga-ohm seals remains low. Thus far, we have used crude manual methods for applying and changing pressures during the clamping process. This results in wide variation in applied pressures while forming the giga-ohm seal and rupturing the membrane for obtaining the whole-cell patch. Naturally, this limits our ability to obtain reproducible conditions

for patching the cell. We can improve the success rate by automating the cell clamping process using computer interfaced syringe pumps. Such automation would also make the assembly amenable to multi-channel recordings for high-throughput electrophysiology for small molecule drug screening (Trepakova, Malik et al. 2007) after suitable modifications to the microfluidic perfusion chamber by electrically isolating individual pores (Lau, Hung et al. 2006; Li, Klemic et al. 2006; John, Dale et al. 2007).

MS channel physiology is still ill-understood. We have provided a versatile tool that could help in plugging the gaps in the current understanding of MS channel physiology as well as pave new avenues in MS channel research. We have also showed that MS channel distribution in HaCaT cells is non-uniform; MS channel activation in HaCaT cells is dependent on the depth of indentation (and thus, dependent on tension in the lipid bilayer); and a threshold tension is necessary to activate MS channels in HaCaT cells. We have partially resolved the role of lipid bilayer tension in activation of MS channels, at least in HaCaT cells. It is generally accepted that MS channel activation is cell-type dependent and similar studies using other cells expressing MS channels might provide a better insight in the general role of lipid bilayer in MS channel activation. Few possible investigative approaches are suggested here:

- Digest sub-membranous cytoskeleton (using chemicals such a cytochlasin D) and study the differences in MS channel activation using direct mechanical stimulus. This could provide a better insight in the role of sub-membranous cytoskeleton and adhesion proteins in MS channel physiology
- Chemically modify bilayer configuration by externally perfusing detergents such lysophosphatidyl choline (LysoPC) and compare the current-voltage characteristics of

before and after this perfusion in cells that are made to heterologously express MS channels but have no native MS channel expression. This approach will help isolate the role of bilayer curvature in MS channel activation

- Indent single cells using microsphere-tagged cantilevers while recording the whole-cell current. Microsphere-tagged cantilevers provide a more distributed stress on the cell, allowing deeper indentations without rupturing the membrane like sharp-tipped cantilevers would. The deeper indentations would incorporate the role of the sub-membranous cytoskeleton in activating MS channels and a comparison between cells with and without (chemically) digested sub-membranous cytoskeleton would give significant insights in the mechanism of activation of MS channels.
- Vary the rate of indentation by the cantilever to study dynamics of MS channel activation.

APPENDIX A

PROCESS PARAMETERS

A double-sided polished oxidized silicon wafer is first subject to a dehydration heating for 90 minutes at 200 ^{o}C. The wafer is then allowed to cool for 10 minutes and immediately used for further processes. The first step is patterning the top-side pores using electron beam lithography, followed by reactive ion etching of the top-side silicon dioxide. This is followed by patterning of the bottom- side pits using photolithography after aligning the pits to corresponding pores on the top-side. The bottom-side oxide is then etched using reactive ion etching followed by isotropic etching of silicon from the bottom-side using XeF_2 etching. The photo-resist and electron-beam resists are then removed by inserting the entire wafer in boiling concentrated sulfuric acid (Piranha clean). The wafer is then subjected a quick O_2 plasma treatment to oxidize the native silicon layer left behind after the dry etch process. Parameters for various microfabrication processes are provided here.

A.1 ELECTRON BEAM LITHOGRAPHY

1. Spin coating (PMMA A4) 30 sec. @ 2000 rpm (0.5 μm thickness)

2. Pre-bake 5 minutes (open hot plate) @ 180 ^{o}C
3. E-beam direct write with a dose of 300 μC/cm^{2}; WD – 5mm; 10 kV; 30 μm aperture
4. Develop PMMA with MIBK (1:3 dilution with 2- Propanol), 30 sec.
5. Rinse in 2-Propanol 5 times, 30 sec. each
6. Post-bake 5 minutes (open hot plate) @ 100 ^{o}C

Observe results using Scanning electron microscopy to ensure the fidelity of features.

A.2 PHOTOLITHOGRAPHY

1. Spin coating (AZ 4210) for 30 sec. @ 3000 rpm (4 μm thickness)
2. Pre-bake 5 minutes (open hot plate) @ 95 ^{o}C
3. Align the mask with the wafer, hard expose 6 sec.
4. Develop (AZ 400K 1:3 dilution in DI water) 30 sec.
5. Rinse in DI water 5 times, 30 sec. each
6. Post-bake 5 minutes (open hot plate) @ 120 ^{o}C

Observe the results of lithography under an optical microscope to ensure the fidelity of the features.

A.3 REACTIVE ION ETCHING

Reactive ion etching is a 1-step process. The wafer is inserted in the reaction chamber. The air from the chamber is pumped out until the pressure in the chamber is 150 mTorr. CF_4 and O_2 are then inserted in the chamber at 45 sccm and 5 sccm respectively. RF power is then switched on at 125 W, to start the reaction. Total reaction time is 465 s to etch the 1 μm oxide. In order to keep the reaction efficiency, the reaction products from the chamber are pumped out every 30 seconds and the reaction gases are re-inserted into the chamber.

A.4 XeF_2 ETCHING

XeF_2 etching is a dry, isotropic technique for etching bulk silicon. Before inserting the sample in the chamber, it is important to remove any residual oxide layer. Silicon dioxide has excellent resistance for XeF_2 etching and any residual oxide with impede silicon etching. Once the residual oxide is removed by a short 15 sec treatment with buffered hydrofluoric acid, the sample is inserted in the chamber. The air from the chamber is then pumped to 50 mTorr and XeF_2 gas is inserted till the pressure rises to 3 Torr. The gases are recycled every 60 seconds. For etching 400 μm silicon, 1200 etching cycles are needed.

A.5 TMAH ETHING

After removing the residual oxide layer with a short 15 second treatment with buffered hydrofluoric acid, the wafer is inserted in 25% TMAH solution @ 90 ^{o}C for 8 hours to etch 400μm silicon. This etching step results in anisotropic pyramidal pit along the <111> crystal planes. Etching is achieved with good surface smoothness. The silicon dioxide acts as an automatic etch-stop.

A.6 BHF ETCHING

The etchant composition is 6:1 by volume of 40% ammonium fluoride (NH_4F) solution (in DI water) to 49 % hydrogen fluoride (HF) in water. The etch rate with this composition is about 2nm/s at 25 celcius.

APPENDIX B

PROTOCOLS AND RECIPES

The section lists the protocols for cell culture and cell isolation procedures and recipes for buffers used for electrophysiology experiments.

B.1 CELL CULTURE

For patch clamp recording, it is important to have cells that are well isolated and have little or no extra-cellular matrix proteins. It becomes especially important to have isolated cells for planar patch clamp given the "blind" choice in the procedure. Hence, for obtaining optimal results, we split the cells before they reached confluence. For CHO and PC12 cells, which grow rapidly, the cells were never left on the plate for longer than 2 days.

HaCaT cells which are relatively slow growing were split every 3 days. HaCaT cells also attach to the substrate very strongly and are therefore, more difficult for automated patch clamp procedures. A longer trypsin treatment is necessary for these cells to obtain the best results.

All cells were cultured in 96 mm diameter culture plates. The incubator was maintained at 37 ^{o}C with 5% CO_2 and 95% relative humidity. The culture media used for cells were:

- CHO cells – F12 media with 10% FCS and 1% penicillin+ streptomyosin+amphotericin (PSA) solution
- PC12 cells – DMEM media with 5% FCS, 10% Horse serum and 1% PSA
- HaCaT cells – DMEM media with 10% FCS and 1% PSA

B.2 CELL ISOLATION

Planar patch clamp involves random choice of a single cell from a cell suspension through application of suction. This makes the procedure essentially a blind approach. Hence, it is imperative that the cells are well isolated to ensure a high success rate. Cell clusters and presence of extracellular debris can clog the pore in the chip, making it useless. In order to isolate the cells (cultured in 96 mm diameter culture plates), the following protocol is followed:

- Wash the cells twice with 10 ml PBS (without Ca^{2+} and Mg^{2+}), 1 minute each
- Add 2 ml of detacher (Trypsin/EDTA)
- Incubate the plate with for 4 minutes @ 37ºC and in 5% CO_2 for detaching the cells
- Check for detachment of cells under an optical microscope. Shake the plate gently to detach all cells from the bottom (do not tap the plate to detach cells)
- Add 10 mL of HEK medium and fetal calf serum (FCS)
- Pipette the suspension from the plate gently up and down with a 10-ml pipette; after pipetting five times, look at the cells under the microscope:
    - If the cells are already single (~80–90%), no further pipetting is necesary

    - If cells are still visible in clusters, gently pipette the suspension another 10 times; repeat this step until cells are single (~80–90%)
- Perform 5 minutes of centrifugation (2000 U/min, 100 g)
- Aspirate out the supernatant
- Resuspend the cells in 10 ml medium with fetal calf serum (FCS).
- Perform 3 minutes of centrifugation (2000 U/min, 100 g).
- Aspirate the supernatant
- Resuspend the cells in ~ 2 ml of external recording solution (resulting in a cell density of approximately $1 \times 10^5 - 5 \times 10^6$/ml medium)

B.3 WHOLE CELL PATCH PROTOCOL

The patch clamp procedure using the planar patch clamp chips differs significantly from traditional micropipette based patch clamp where a cell is chosen by observing under an optical microscope and a micropipette is maneuvered towards it using a micro-manipulator. The planar patch clamp chip based protocol is a blind approach where cell suspension is placed on top of the chip and a cell is patched on to the pore by application of suction:

- Fill the bottom reservoir of the perfusion chamber with appropriate intra-cellular buffer, make sure that there are no air bubbles in the reservoir or feed lines
- Wet the chip pore from the bottom side using the intra-cellular buffer and place the chip on the bottom reservoir
- Place the Ag/AgCl electrodes in the corresponding feed lines on top and bottom halves and connect to the patch clamp amplifier

- Screw the top half of the perfusion chamber on to the bottom reservoir; ensure that the O-rings on both the top half and the bottom reservoir are in their slots and that the solution is not leaking through
- Switch on the patch clamp amplifier and adjust the settings according to the experiment
- Gently drop the cell suspension near the center of the chip using a 200 µl pipette
- While the cells settle for about 30 seconds, apply a gentle pressure from the bottom side to keep any possible small particle contaminants away from the pore
- Using the syringe attached to the feed lines on the bottom reservoir, apply a gentle suction to draw cells towards the pore; monitor the resistance across the pore
- Stop the suction when the resistance saturates to a value higher than 600 MΩ; if the saturation resistance value is significantly smaller than 600 MΩ, discard the chip and start over (smaller saturation resistance signals bad seal making the chip useless)
- Apply a sharp, suction pulse using the feed lines and syringe to rupture the patch of membrane enclosed within the pore; this gives access to the inside of the cell forming a whole-cell-patch – the resistance at this stage should drop to few 10s of MΩs

BIBLIOGRAPHY

Akitake, B., A. Anishkin, et al. (2005). "The "dashpot" mechanism of stretch-dependent gating in MscS." J Gen Physiol **125**(2): 143-54.

Alessandri-Haber, N., E. Joseph, et al. (2005). "TRPV4 mediates pain-related behavior induced by mild hypertonic stimuli in the presence of inflammatory mediator." Pain **118**(1-2): 70-9.

Alessandri-Haber, N., J. J. Yeh, et al. (2003). "Hypotonicity induces TRPV4-mediated nociception in rat." Neuron **39**(3): 497-511.

Andrade, Y. N., J. Fernandes, et al. (2005). "TRPV4 channel is involved in the coupling of fluid viscosity changes to epithelial ciliary activity." J Cell Biol **168**(6): 869-74.

Armstrong, C. M., R. P. Swenson, Jr., et al. (1982). "Block of squid axon K channels by internally and externally applied barium ions." J Gen Physiol **80**(5): 663-82.

Becker, D., C. Blase, et al. (2005). "TRPV4 exhibits a functional role in cell-volume regulation." J Cell Sci **118**(Pt 11): 2435-40.

Betanzos, M., C. S. Chiang, et al. (2002). "A large iris-like expansion of a mechanosensitive channel protein induced by membrane tension." Nat Struct Biol **9**(9): 704-10.

Blount, P., S. I. Sukharev, et al. (1996). "Towards an understanding of the structural and functional properties of MscL, a mechanosensitive channel in bacteria." Biol Cell **87**(1-2): 1-8.

Bourque, C. W., S. H. Oliet, et al. (1994). "Osmoreceptors, osmoreception, and osmoregulation." Front Neuroendocrinol **15**(3): 231-74.

Cahalan, M. D. and K. G. Chandy (1997). "Ion channels in the immune system as targets for immunosuppression." Curr Opin Biotechnol **8**(6): 749-56.

Candiello, J., M. Balasubramani, et al. (2007). "Biomechanical properties of native basement membranes." FEBS J **274**(11): 2897-908.

Chen, C. and A. Folch (2006). "A high-performance elastomeric patch clamp chip." Lab Chip **6**(10): 1338-45.

Chiang, C. S., A. Anishkin, et al. (2004). "Gating of the large mechanosensitive channel in situ: estimation of the spatial scale of the transition from channel population responses." Biophys J **86**(5): 2846-61.

Chung, M. K., H. Lee, et al. (2003). "Warm temperatures activate TRPV4 in mouse 308 keratinocytes." J Biol Chem **278**(34): 32037-46.

Corey, D. P., J. Garcia-Anoveros, et al. (2004). "TRPA1 is a candidate for the mechanosensitive transduction channel of vertebrate hair cells." Nature **432**(7018): 723-30.

Cui, C., D. O. Smith, et al. (1995). "Characterization of mechanosensitive channels in Escherichia coli cytoplasmic membrane by whole-cell patch clamp recording." J Membr Biol **144**(1): 31-42.

Davis, M. J., J. A. Donovitz, et al. (1992). "Stretch-activated single-channel and whole cell currents in vascular smooth muscle cells." Am J Physiol **262**(4 Pt 1): C1083-8.

Dichter, M. A., A. S. Tischler, et al. (1977). "Nerve growth factor-induced increase in electrical excitability and acetylcholine sensitivity of a rat pheochromocytoma cell line." Nature **268**(5620): 501-4.

Dieluweit, S., A. Csiszar, et al. (2010). "Mechanical Properties of Bare and Protein-Coated Giant Unilamellar Phospholipid Vesicles. A Comparative Study of Micropipet Aspiration and Atomic Force Microscopy." Langmuir.

Evans, E. and D. Needham (1986). "Giant vesicle bilayers composed of mixtures of lipids, cholesterol and polypeptides. Thermomechanical and (mutual) adherence properties." Faraday Discuss Chem Soc(81): 267-80.

Fertig, N., R. H. Blick, et al. (2002). "Whole cell patch clamp recording performed on a planar glass chip." Biophys J **82**(6): 3056-62.

Fertig, N., M. George, et al. (2003). "Microstructured apertures in planar glass substrates for ion channel research." Receptors Channels **9**(1): 29-40.

Fertig, N., C. Meyer, et al. (2001). "Microstructured glass chip for ion channel electrophysiology." Phys Rev E (rapid communications) **64**.

Furness, D. N., A. Karkanevatos, et al. (2002). "An immunogold investigation of the distribution of calmodulin in the apex of cochlear hair cells." Hear Res **173**(1-2): 10-20.

Gamper, N., J. D. Stockand, et al. (2005). "The use of Chinese hamster ovary (CHO) cells in the study of ion channels." J Pharmacol Toxicol Methods **51**(3): 177-85.

Guler, A. D., H. Lee, et al. (2002). "Heat-evoked activation of the ion channel, TRPV4." J Neurosci **22**(15): 6408-14.

Hamill, O. P., Ed. (2007). Mechanosensitive Ion Channels, Part A. Current Topics in Membranes, Academic Press.

Hamill, O. P. and D. W. McBride, Jr. (1997). "Induced membrane hypo/hyper-mechanosensitivity: a limitation of patch-clamp recording." Annu Rev Physiol **59**: 621-31.

Hartmannsgruber, V., W. T. Heyken, et al. (2007). "Arterial response to shear stress critically depends on endothelial TRPV4 expression." PLoS ONE **2**(9): e827.

Hille, B. (2001). Ion Channels of Excitable Membranes, Sinauer Associates, Massachussetts.

Horber, J. K., J. Mosbacher, et al. (1995). "A look at membrane patches with a scanning force microscope." Biophys J **68**(5): 1687-93.

Hoshi, T. and R. W. Aldrich (1988). "Voltage-dependent K+ currents and underlying single K+ channels in pheochromocytoma cells." J Gen Physiol **91**(1): 73-106.

Hughes, S., A. J. El Haj, et al. (2005). "Magnetic micro- and nanoparticle mediated activation of mechanosensitive ion channels." Med Eng Phys **27**(9): 754-62.

Hughes, S., S. McBain, et al. (2007). "Selective activation of mechanosensitive ion channels using magnetic particles." J R Soc Interface.

Ingber, D. E. (1997). "Tensegrity: the architectural basis of cellular mechanotransduction." Annu Rev Physiol **59**: 575-99.

Ingber, D. E. (2006). "Cellular mechanotransduction: putting all the pieces together again." FASEB J **20**(7): 811-27.

Ionescu-Zanetti, C., R. M. Shaw, et al. (2005). "Mammalian electrophysiology on a microfluidic platform." Proc Natl Acad Sci U S A **102**(26): 9112-7.

Janigro, D., G. Maccaferri, et al. (1989). "Calcium channels in undifferentiated PC12 rat pheochromocytoma cells." FEBS Lett **255**(2): 398-400.

Jeon, J. and G. A. Voth (2008). "Gating of the mechanosensitive channel protein MscL: the interplay of membrane and protein." Biophys J **94**(9): 3497-511.

Jia, Y., X. Wang, et al. (2004). "Functional TRPV4 channels are expressed in human airway smooth muscle cells." Am J Physiol Lung Cell Mol Physiol **287**(2): L272-8.

John, V. H., T. J. Dale, et al. (2007). "Novel 384-well population patch clamp electrophysiology assays for Ca2+-activated K+ channels." J Biomol Screen **12**(1): 50-60.

Kamkin, A., I. Kiseleva, et al. (2003). "Activation and inactivation of a non-selective cation conductance by local mechanical deformation of acutely isolated cardiac fibroblasts." Cardiovasc Res **57**(3): 793-803.

Kamkin, A., I. Kiseleva, et al. (2003). "Ion selectivity of stretch-activated cation currents in mouse ventricular myocytes." Pflugers Arch **446**(2): 220-31.

Kamkin, A., I. Kiseleva, et al. (2005). "Electrical interaction of mechanosensitive fibroblasts and myocytes in the heart." Basic Res Cardiol **100**(4): 337-45.

Klemic, K. G., J. F. Klemic, et al. (2002). "Micromolded PDMS planar electrode allows patch clamp electrical recordings from cells." Biosens Bioelectron **17**(6-7): 597-604.

Klemic, K. G., J. F. Klemic, et al. (2005). "An air-molding technique for fabricating PDMS planar patch-clamp electrodes." Pflugers Arch **449**(6): 564-72.

Kloda, A. and B. Martinac (2001). "Molecular identification of a mechanosensitive channel in archaea." Biophys J **80**(1): 229-40.

Koitschev, A., S. Fink, et al. (2002). "[Atomic force microscope (AFM). A nanomanipulator for biophysical studies of stereocilia of the cochlear hair cells]." HNO **50**(5): 464-9.

Kwon, E.-Y. K., Young-Tae; Kim, Dae-Eun (2009). " Investigation of penetration force of living cell using an atomic force microscope." Journal of Mechanical Science and Technology **23**: 1932-1938.

Lal, R., H. Kim, et al. (1993). "Imaging of reconstituted biological channels at molecular resolution by atomic force microscopy." Am J Physiol **265**(3 Pt 1): C851-6.

Lal, R. and H. Lin (2001). "Imaging molecular structure and physiological function of gap junctions and hemijunctions by multimodal atomic force microscopy." Microsc Res Tech **52**(3): 273-88.

Langer, M. G., A. Koitschev, et al. (2000). "Mechanical stimulation of individual stereocilia of living cochlear hair cells by atomic force microscopy." Ultramicroscopy **82**(1-4): 269-78.

Larmer, J., S. W. Schneider, et al. (1997). "Imaging excised apical plasma membrane patches of MDCK cells in physiological conditions with atomic force microscopy." Pflugers Arch **434**(3): 254-60.

Lau, A. Y., P. J. Hung, et al. (2006). "Open-access microfluidic patch-clamp array with raised lateral cell trapping sites." Lab Chip **6**(12): 1510-5.

Li, X., K. G. Klemic, et al. (2006). "Microfluidic system for planar patch clamp electrode arrays." Nano Lett **6**(4): 815-9.

Liedtke, W., Y. Choe, et al. (2000). "Vanilloid receptor-related osmotically activated channel (VR-OAC), a candidate vertebrate osmoreceptor." Cell **103**(3): 525-35.

Liedtke, W. and J. M. Friedman (2003). "Abnormal osmotic regulation in trpv4-/- mice." Proc Natl Acad Sci U S A **100**(23): 13698-703.

Liedtke, W., D. M. Tobin, et al. (2003). "Mammalian TRPV4 (VR-OAC) directs behavioral responses to osmotic and mechanical stimuli in Caenorhabditis elegans." Proc Natl Acad Sci U S A **100 Suppl 2**: 14531-6.

Lin, H., R. Bhatia, et al. (2001). "Amyloid beta protein forms ion channels: implications for Alzheimer's disease pathophysiology." FASEB J **15**(13): 2433-44.

Lin, H., D. O. Clegg, et al. (1999). "Imaging real-time proteolysis of single collagen I molecules with an atomic force microscope." Biochemistry **38**(31): 9956-63.

Mangos, S., Y. Liu, et al. (2007). "Dynamic expression of the osmosensory channel trpv4 in multiple developing organs in zebrafish." Gene Expr Patterns **7**(4): 480-4.

Martinac, B., M. Buechner, et al. (1987). "Pressure-sensitive ion channel in Escherichia coli." Proc Natl Acad Sci U S A **84**(8): 2297-301.

Mayer, M., J. K. Kriebel, et al. (2003). "Microfabricated teflon membranes for low-noise recordings of ion channels in planar lipid bilayers." Biophys J **85**(4): 2684-95.

McBride, D. W., Jr. and O. P. Hamill (1992). "Pressure-clamp: a method for rapid step perturbation of mechanosensitive channels." Pflugers Arch **421**(6): 606-12.

McBride, D. W., Jr. and O. P. Hamill (1993). "Pressure-clamp technique for measurement of the relaxation kinetics of mechanosensitive channels." Trends Neurosci **16**(9): 341-5.

Merryman, W. D., J. Liao, et al. (2007). "Differences in tissue-remodeling potential of aortic and pulmonary heart valve interstitial cells." Tissue Eng **13**(9): 2281-9.

Mizoguchi, F., A. Mizuno, et al. (2008). "Transient receptor potential vanilloid 4 deficiency suppresses unloading-induced bone loss." J Cell Physiol.

Neher, E. and B. Sakmann (1976). "Noise analysis of drug induced voltage clamp currents in denervated frog muscle fibres." J Physiol **258**(3): 705-29.

Neher, E. and B. Sakmann (1976). "Single-channel currents recorded from membrane of denervated frog muscle fibres." Nature **260**(5554): 799-802.

Nilius, B., J. Prenen, et al. (2001). "Differential activation of the volume-sensitive cation channel TRP12 (OTRPC4) and volume-regulated anion currents in HEK-293 cells." Pflugers Arch **443**(2): 227-33.

Nilius, B., J. Vriens, et al. (2004). "TRPV4 calcium entry channel: a paradigm for gating diversity." Am J Physiol Cell Physiol **286**(2): C195-205.

Obataya, I., C. Nakamura, et al. (2005). "Mechanical sensing of the penetration of various nanoneedles into a living cell using atomic force microscopy." Biosens Bioelectron **20**(8): 1652-5.

Okada, K., P. C. Moe, et al. (2002). "Functional design of bacterial mechanosensitive channels. Comparisons and contrasts illuminated by random mutagenesis." J Biol Chem **277**(31): 27682-8.

Opsahl, L. R. and W. W. Webb (1994). "Lipid-glass adhesion in giga-sealed patch-clamped membranes." Biophys J **66**(1): 75-9.

Pamir, E., M. George, et al. (2007). "Planar patch-clamp force microscopy on living cells." Ultramicroscopy.

Pantoja, R., J. M. Nagarah, et al. (2004). "Silicon chip-based patch-clamp electrodes integrated with PDMS microfluidics." Biosens Bioelectron **20**(3): 509-17.

Perozo, E., A. Kloda, et al. (2002). "Physical principles underlying the transduction of bilayer deformation forces during mechanosensitive channel gating." Nat Struct Biol **9**(9): 696-703.

Quist, A. P., A. Chand, et al. (2007). "Atomic force microscopy imaging and electrical recording of lipid bilayers supported over microfabricated silicon chip nanopores: lab-on-a-chip system for lipid membranes and ion channels." Langmuir **23**(3): 1375-80.

Rae, J., K. Cooper, et al. (1991). "Low access resistance perforated patch recordings using amphotericin B." J Neurosci Methods **37**(1): 15-26.

Reiter, B., R. Kraft, et al. (2006). "TRPV4-mediated regulation of epithelial permeability." FASEB J **20**(11): 1802-12.

Roiter, Y. and S. Minko (2005). "AFM single molecule experiments at the solid-liquid interface: in situ conformation of adsorbed flexible polyelectrolyte chains." J Am Chem Soc **127**(45): 15688-9.

Schmidt, C., M. Mayer, et al. (2000). "A Chip-Based Biosensor for the Functional Analysis of Single Ion Channels " Angew Chem Int Ed Engl **39**(17): 3137-3140.

Schoenmakers, T. J., H. Vaudry, et al. (1995). "Osmo- and mechanosensitivity of the transient outward K+ current in a mammalian neuronal cell line." J Physiol **489 (Pt 2)**: 419-30.

Sigworth, F. J. and K. G. Klemic (2005). "Microchip technology in ion-channel research." IEEE Trans Nanobioscience **4**(1): 121-7.

Sipe, W., S. M. Brierley, et al. (2008). "Transient Receptor Potential Vanilloid 4 Mediates Protease Activated Receptor 2-Induced Sensitization of Colonic Afferent Nerves and Visceral Hyperalgesia." Am J Physiol Gastrointest Liver Physiol.

Stett, A., V. Bucher, et al. (2003). "Patch-clamping of primary cardiac cells with micro-openings in polyimide films." Med Biol Eng Comput **41**(2): 233-40.

Stett, A., C. Burkhardt, et al. (2003). "CYTOCENTERING: a novel technique enabling automated cell-by-cell patch clamping with the CYTOPATCH chip." Receptors Channels **9**(1): 59-66.

Suchyna, T. M., V. S. Markin, et al. (2009). "Biophysics and structure of the patch and the gigaseal." Biophys J **97**(3): 738-47.

Sukharev, S. (2002). "Purification of the small mechanosensitive channel of Escherichia coli (MscS): the subunit structure, conduction, and gating characteristics in liposomes." Biophys J **83**(1): 290-8.

Sukharev, S., M. Betanzos, et al. (2001). "The gating mechanism of the large mechanosensitive channel MscL." Nature **409**(6821): 720-4.

Sukharev, S., S. R. Durell, et al. (2001). "Structural models of the MscL gating mechanism." Biophys J **81**(2): 917-36.

Sukharev, S. I., B. Martinac, et al. (1993). "Two types of mechanosensitive channels in the Escherichia coli cell envelope: solubilization and functional reconstitution." Biophys J **65**(1): 177-83.

Suzuki, M., A. Mizuno, et al. (2003). "Impaired pressure sensation in mice lacking TRPV4." J Biol Chem **278**(25): 22664-8.

Tabuchi, K., M. Suzuki, et al. (2005). "Hearing impairment in TRPV4 knockout mice." Neurosci Lett **382**(3): 304-8.

Tang, X. D., R. Xu, et al. (2003). "Haem can bind to and inhibit mammalian calcium-dependent Slo1 BK channels." Nature **425**(6957): 531-5.

Taniguchi, J., S. Tsuruoka, et al. (2007). "TRPV4 as a flow sensor in flow-dependent K+ secretion from the cortical collecting duct." Am J Physiol Renal Physiol **292**(2): F667-73.

Trepakova, E. S., M. G. Malik, et al. (2007). "Application of PatchXpress Planar Patch Clamp Technology to the Screening of New Drug Candidates for Cardiac KCNQ1/KCNE1 (I(Ks)) Activity." Assay Drug Dev Technol.

Waniishi, Y., R. Inoue, et al. (1997). "Preferential potentiation by hypotonic cell swelling of muscarinic cation current in guinea pig ileum." Am J Physiol **272**(1 Pt 1): C240-53.

Watanabe, H., J. B. Davis, et al. (2002). "Activation of TRPV4 channels (hVRL-2/mTRP12) by phorbol derivatives." J Biol Chem **277**(16): 13569-77.

Watanabe, H., J. Vriens, et al. (2003). "Anandamide and arachidonic acid use epoxyeicosatrienoic acids to activate TRPV4 channels." Nature **424**(6947): 434-8.

Watanabe, H., J. Vriens, et al. (2002). "Heat-evoked activation of TRPV4 channels in a HEK293 cell expression system and in native mouse aorta endothelial cells." J Biol Chem **277**(49): 47044-51.

Wu, L., X. Gao, et al. (2007). "Dual Role of the Trpv4 Channel as a Sensor of Flow and Osmolality in Renal Epithelial Cells." Am J Physiol Renal Physiol.

Xian Tao, L., V. Dyachenko, et al. (2006). "The stretch-activated potassium channel TREK-1 in rat cardiac ventricular muscle." Cardiovasc Res **69**(1): 86-97.

Xu, J., A. Guia, et al. (2003). "A benchmark study with sealchip planar patch-clamp technology." Assay Drug Dev Technol **1**(5): 675-84.

Zhang, P. C., A. M. Keleshian, et al. (2001). "Voltage-induced membrane movement." Nature **413**(6854): 428-32.